Title
KINETICS OF NITROGEN DIOXIDE FLUORESCENCE

Authors
Schwartz, Stephen E.
Johnston, Harold S.

Publication Date
1969-04-01

Submitted to the Journal
of Chemical Physics

UCRL-18431 Rev.
Preprint

cy. 2

KINETICS OF NITROGEN DIOXIDE FLUORESCENCE

Stephen E. Schwartz and Harold S. Johnston

April 1969

AEC Contract No. W-7405-eng-48

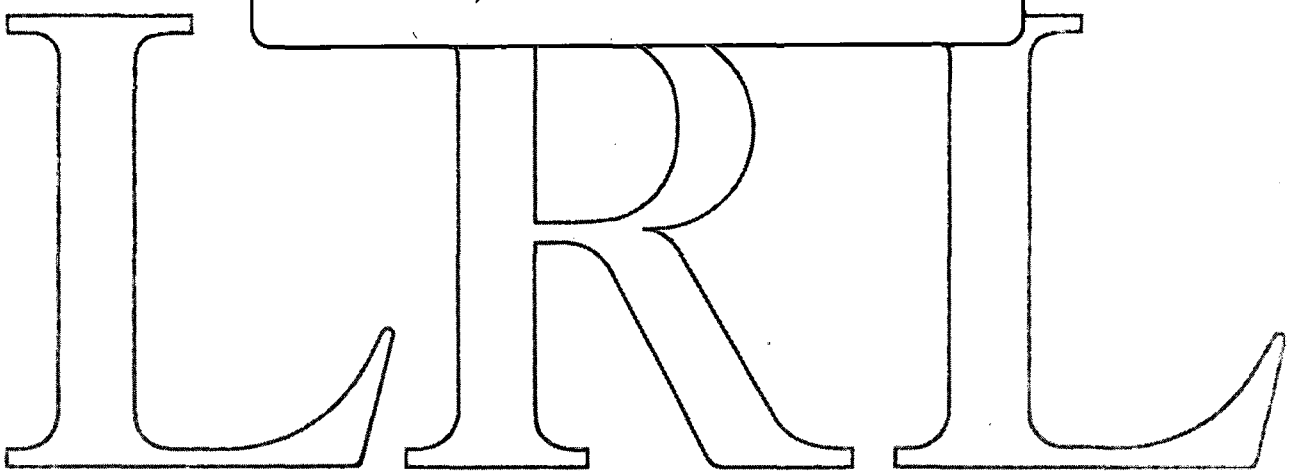

LAWRENCE RADIATION LABORATORY
UNIVERSITY of CALIFORNIA BERKELEY

cy. 2

UCRL-18431 Rev.

DISCLAIMER

KINETICS OF NITROGEN DIOXIDE FLUORESCENCE[1]

Stephen E. Schwartz* and Harold Johnston

Inorganic Materials Research Division, Lawrence Radiation Laboratory,
and Department of Chemistry,
University of California, Berkeley, California

ABSTRACT

The fluorescence lifetime and intensity of gas phase nitrogen dioxide ($^2B_1$) have been measured as a function of excitation wavelength, fluorescence wavelength, and pressure (0.5 to 50 mtorr). The phase-shift method was used; this technique allows lifetime measurements to be obtained with signal intensities of 100 counts per second and lower. The excitation source, tunable throughout the visible region, had a half-width bandpass as low as 15 A. Fluorescence wavelength separation was accomplished with 15 interference filters between 4000 and 8000 A. The radiative lifetimes range from 55 to 90 μsec for excitation from 3980 to 6000 A, and tend to increase with excitation wavelength; however, the lifetimes exhibit considerable variation within a narrow excitation region.

The fluorescence sample was contained in a 33 cm diameter spherical bulb; apparent fluorescence lifetimes in smaller cells were reduced because of migration of excited molecules (under collision-free conditions) and wall quenching. In order that the measured lifetime exhibit no more than 5% error, observation must be extended beyond the excitation region to a distance 5 times the product of the lifetime by the most probable velocity.

---

* Present address: Department of Physical Chemistry, Cambridge, England.
NSF Graduate Student Fellowship, 1964-1968.

The Stern-Volmer analysis of fluorescence kinetics has been generalized to a multi-level system under conditions of modulated excitation and phase-sensitive detection. Analysis of fluorescence data in terms of this mechanism yields the product of energy-transfer rate constants times efficiencies (amount of energy lost by the excited polyatomic molecule per effective collision). This analysis implies the loss of at least one vibrational quantum (average value 1230 cm^{-1}) per gas-kinetic collision over the entire range from 12500 to 25000 cm^{-1} energy above the ground state. This result indicates that molecules in the $^2B_1$ excited electronic state are rapidly interconverted to the high vibrational levels of the ground electronic state.

INTRODUCTION

Fluorescence has been widely used as an analytical technique in the study of energy transfer processes of molecules.[2] This technique is capable of providing detailed information about the nature of energy transfer processes which are undergone by excited molecules since it allows for direct spectral observation of the populations of the various quantum states.[3] In addition, time-resolved fluorescence studies allow direct measurement of radiative and energy transfer processes.[4]

The present study is a time-resolved investigation of the kinetics of NO_2 fluorescence excited by visible radiation ($X\,^2A_1 \leftarrow A\,^2B_1$) and of the energy transfer process of the excited molecules. Nitrogen dioxide was selected as the subject of such a study because:

1) Very little quantitative information exists about the rates and efficiencies of energy transfer processes in highly excited small polyatomic molecules, and there are no direct measurements of these processes in triatomic molecules. Previous studies of fluorescence quenching have indicated that energy transfer processes involving NO_2 ($^2B_1$) take place with high probability,[5] and that such processes may take place by a stepwise mechanism.[6]

2) There have been recent doubts concerning the validity of the existing value of the radiative lifetime of NO_2 ($^2B_1$), 44 μsec,[5,7] which is anomalously long for an allowed electronic transition. No dependence of the lifetime upon the energy of the excited molecule has previously been reported, although such

a dependence may be expected from the $\tilde{\nu}^3$ factor in the Einstein A coefficient[8] and from the existence of strong perturbations in the upper state.[9]

3) Radiation of NO_2 is an elementary process in the NO + O and NO + O_3 chemiluminescence reactions, which have received considerable study in the laboratory and, in the former case, as an upper atmosphere reaction.[16,17] Any understanding of the rates of radiative and non-radiative processes that is obtained from fluorescence studies can be used to increase our understanding of the chemical processes responsible for the population and depopulation of the excited electronic state in these specific reactions.

4) NO_2 is advantageous from an experimental point of view, having an electronic transition in a spectral region well suited to investigation. The upper state of this transition is presumed to be the lowest excited electronic state on the basis of theoretical considerations[18] and of a partial rotational analysis of the absorption spectrum.[9] Consequently, relaxation studies are probably not complicated by the presence of other electronic states.

THEORY OF MEASUREMENTS

A. Linear, one-state mechanism

The theory of the phase-shift technique of lifetime measurements has been developed by previous investigators.[4,19-21] The simplest linear mechanism involving a single excited species

is

$$G + h\nu_x \xrightarrow{a} E \qquad (1)$$

$$E \xrightarrow{k} \ldots$$

where a is the absorption cross section, G represents ground state molecules, ν_x, is the frequency of excitation, and k is the first-order rate constant for disappearance of the excited species. If the intensity of exciting radiation, I_x, is modulated sinusoidally with angular frequency ω

$$I_x = I_o \exp(i\,\omega\,t) \qquad (2)$$

the concentration of excited species varies as

$$E(t) = \frac{a\,G\,I_x}{k + i\,\omega} = \frac{a\,G\,I_x}{k^2 + \omega^2}(k - i\,\omega) \qquad (3)$$

The measured fluorescence signal is given by

$$S(t) = \alpha\, f\, E \qquad (4)$$

where α is the combined optical collection and detection efficiency, and f is the rate constant for fluorescence ($f \leq k$).

The modulated concentration E and detected signal S may be formally expressed in terms of components in-phase and -90 degrees out-of-phase with the exciting radiation

$$E = E_o - i\,E_{-90} \qquad (5)$$

$$S = S_o - i\,S_{-90} \qquad (6)$$

In the experiments reported here, the directly observed quantities are S_o and S_{-90}. We define, measure, and tabulate two

functions of the observed signal components

$$\underline{R} = S_{-90} / S_o \qquad (7)$$

$$\underline{I} = \frac{(S_o)^2 + (S_{-90})^2}{S_o} \qquad (8)$$

These composite, observable functions, R and I, have definite physical interpretations in terms of various molecular models for the fluorescing system.

In the general linear mechanism given by (1), the differential equation for the excited species is

$$\frac{dE}{dt} = \underline{a}\, G\, I_x - \underline{k}\, E \qquad (9)$$

For steady-state illumination at intensity I_o, the concentration of the excited species is $\underline{a}\, G\, I_o / \underline{k}$, and the observed fluorescence intensity is $\alpha\, \underline{f}\, \underline{a}\, G\, I_o / \underline{k}$. For a flash-decay experiment the excited species disappears (after the flash is quenched) as $E_{max} \exp(-\underline{k}\, t)$. A comparison of (3), (5), (6), (7), and (8) with these relations shows that the observed function $\underline{R}$ is closely related to the lifetime τ of the excited species as it would be measured in a flash-decay experiment

$$\tau = \frac{1}{\underline{k}} = \frac{R}{\omega} \qquad (10)$$

and the observed function $\underline{I}$ is the fluorescence intensity that would be measured in a steady or dc illumination

$$\underline{I} = \frac{\alpha\, \underline{f}\, \underline{a}\, G\, I_o}{\underline{k}} = \alpha\, \underline{f}\, E_{ss} = \underline{I}_{ss} \qquad (11)$$

It is convenient to normalize the intensity $\underline{I}$ by the concentration of ground-state molecules and to define the normalized intensity $\underline{J}$

$$\underline{J} = \underline{I} / G \tag{12}$$

B. Stern-Volmer Mechanism of Fluorescence Quenching

According to the Stern-Volmer[22,23] mechanism, the exicted species are removed by collisional deactivation in addition to fluorescence

$$E \xrightarrow{f} h\nu_f + G \tag{13}$$

$$E + M \xrightarrow{q} M + G$$

In this case the general first-order rate constant $\underline{k}$ is $\underline{f} + \underline{q}\ M$, and this relation may be substituted into the lifetime expression (10) and the intensity expressions (11) and (12). With the Stern-Volmer model there are four different plots that should be linear. Two are useful for extrapolation to zero quenching pressure

$$\omega / \underline{R} = \underline{f} + \underline{q}\ M \tag{14}$$

$$\underline{J}^{-1} = (\alpha\ \underline{a}\ I_o)^{-1} (1 + \frac{\underline{q}}{\underline{f}} M) \tag{15}$$

and two are useful for extrapolation to infinite pressure

$$\omega / \underline{R}\ M = \underline{q} + \underline{f}\ M^{-1} \tag{16}$$

$$(\underline{J}\ M)^{-1} = (\alpha\ \underline{a}\ I_o)^{-1} (\frac{\underline{q}}{\underline{f}} + M^{-1}) \tag{17}$$

The lifetime plots give the separate terms, q and f, but the intensity plots give only the ratio q / f.

C. General Model[24] of Energy Transfer in Excited NO_2

The interpretation of the results of the pressure-dependent studies is developed in terms of a mechanism in which certain quantum states of the molecule are initially populated optically and additional states are subsequently populated as energy is removed from the excited molecule upon collisions with heat-bath molecules. This mechanism is expressed with full generality in terms of a set of linear differential equations for the population in each quantum state j.

$$\frac{d E_j}{dt} = I_x G a_j - E_j f_j - M E_j q_j + M \sum_p q_{jp} E_p \qquad (18)$$

where a_j is the absorption cross section into state j, f_j is the rate constant for fluorescence from state j, q_{jp} is the microscopic energy-transfer rate constant from state p into state j, and $q_j = \sum_p q_{pj}$, the total rate constant for collisional removal from state j. Neglecting transient terms, we obtain for sinusoidal excitation at the angular frequency ω the set of algebraic equations

$$\left(q_j + \frac{f_j}{M} + \frac{i \omega}{M} \right) E_j - \sum_p q_{jp} E_p = \frac{I_o G}{M} a_j \qquad (19)$$

These equations may be written in compact matrix notation

$$(\underset{\sim}{C} + \frac{\underset{\sim}{F}}{M} + \frac{i\omega}{M}\ \underset{\sim}{1})\ \underset{\sim}{E} = \frac{I_o G}{M}\ \underset{\sim}{A} \qquad (20)$$

where $\underset{\sim}{E}$ is the column vector of the populations,

$\underset{\sim}{A}$ is the column vector of absorption coefficients

$\underset{\sim}{F}$ is the diagonal matrix of fluorescence rate constants,

and

$\underset{\sim}{C}$ is the matrix of quenching rate constants

$$\underset{\sim}{C} = \begin{pmatrix} q_1 & -q_{12} & -q_{13} & \cdots \\ -q_{21} & q_2 & -q_{23} & \cdots \\ -q_{31} & -q_{32} & q_3 & \cdots \\ \cdot & \cdot & \cdot & \cdots \end{pmatrix}$$

We may use (20) to demonstrate the existence of high pressure limits in fluorescence kinetics. The matrix of the populations may be written as the sum of real (in-phase) and imaginary (quadrature) components.

$$\underset{\sim}{E} = \underset{\sim}{E}_o - i\,\underset{\sim}{E}_{-90} \qquad (21)$$

From (20) and (21) we obtain

$$(M\,\underset{\sim}{C} + \underset{\sim}{F})\ \underset{\sim}{E}_o + \omega\,\underset{\sim}{E}_{-90} = I_o G\,\underset{\sim}{A} \qquad (22)$$

$$(M\,\underset{\sim}{C} + \underset{\sim}{F})\ \underset{\sim}{E}_{-90} - \omega\,\underset{\sim}{E}_o = 0$$

At high pressures the in-phase and quadrature components become

$$\underset{\sim}{E}_o = \frac{I_o G}{M}\ \underset{\sim}{C}^{-1}\ \underset{\sim}{A} \qquad (23)$$

$$\underset{\sim}{E}_{-90} = \frac{I_o G \omega}{M^2}\ \underset{\sim}{C}^{-2}\ \underset{\sim}{A}$$

Thus it is shown that the vectors of both the in-phase and quadrature populations reach constant limits which have respectively inverse first order and inverse second order dependence on the total pressure. The populations in the various quantum states reach a limiting, relative distribution, which is dependent on the energy of excitation and the microscopic rate constants connecting the various states but is independent of the total pressure. As a consequence of this constant distribution function, the spectra of the observed signals, $S_{/o}$ and $S_{/-90}$, become independent of pressure except for a constant factor, that is, the spectra of log $S_{/o}$ or log $S_{/-90}$ will attain a shape that is the same for all high pressures. From (23) it may be seen that the linear-kinetics quantities, (10), (11), and (12), for each quantum state $\underline{j}$ reach high-pressure limits. In terms of the components of the populations of the excited states j, it is convenient to define the high-pressure quenching constant

$$\underline{Q}_j = \lim_{M \to \infty} \frac{\omega}{M \underline{R}_j} = \omega \frac{\lim M \underline{E}_{/oj}}{\lim M^2 \underline{E}_{/-90j}} \qquad (24)$$

and to define the limiting high-pressure intensity

$$\underline{Y}_j = \lim_{M \to \infty} M \underline{I}_j \qquad (25)$$

Spectra of the quantities, (24) and (25), in arbitrary resolution, attain at high pressures a shape that is independent of pressure.

D. Step-ladder Model of Energy Transfer in Excited NO_2

The general model discussed above is very useful in proving general theorems, such as the existence of the high-pressure limits (23-25). A simplified version, which can be solved in terms of observable data, is the step-ladder model as used by Rabinovitch and coworkers,[25] expressed here in the terms of the Rice-Ramsperger-Kassel (RRK) theory of unimolcular reactions.[26] In this case the energy step-size ϵ is appropriately taken as the average of the normal-mode frequencies, and the multiplicity of an energy level is given by a simple closed formula

$$g_j = \frac{(j + s - 1)!}{j!\,(s - 1)!} \tag{26}$$

$j\,\epsilon$ = total vibrational energy

s = number of normal modes of vibration

We may index the vibrational energy levels of the molecule as $0 \ldots j \ldots p$, where p is the index of the optically populated state, and j is a running index between zero and p. The set of differential equations in terms of energy levels is

$$\frac{d E_p}{d t} = a_p G I_x - (b_p M + q_p M + f_p) E_p \tag{27}$$

$$\frac{d E_{p-1}}{d t} = b_p M E_p - (b_{p-1} M + q_{p-1} M + f_{p-1}) E_{p-1}$$

$$\frac{d E_j}{d t} = b_{j+1} M E_{j+1} - (b_j M + q_j M + f_j) E_j$$

where $\underline{f}$ is the fluorescence rate constant, $\underline{b}$ is the vibrational quenching constant, and $\underline{q}$ is the electronic quenching constant. (This mechanism omits the possibility of "back-up" collisions). For sinusoidal excitation (2) this set of equations can be solved for the population of excited molecules in a particular energy level $\underline{n}$

$$E_{\underline{n}}(t) = a_{\underline{p}} G I_x \frac{\prod_{j=\underline{n}+1}^{p} b_j M}{\prod_{j=\underline{n}}^{p} (b_j M + q_j M + f_j + i\omega)} \qquad (28)$$

At the high-pressure limit where $(b_j M + q_j M) \gg f_j$, the expression for the population is

$$E_{\underline{n}} = \frac{a_{\underline{p}} G I_x}{M} \frac{\prod_{\underline{n}+1}^{p} b_j}{\prod_{\underline{n}}^{p} (b_j + q_j)} \left(1 - \frac{i\omega}{M} \sum_{\underline{n}}^{p} \frac{1}{b_j + q_j}\right) \qquad (29)$$

In terms of this mechanism the observable high-pressure quenching constant Q (24) is given by

$$Q_{\underline{n}}^{-1} = \sum_{\underline{n}}^{p} (b_j + q_j)^{-1} \qquad (30)$$

The high-pressure limiting population (in pure NO_2 where M is G) is

$$P_n = a_p I_o \frac{\prod_{n+1}^{p} b_j}{\prod_{n}^{p} (b_j + q_j)} \qquad (31)$$

In these multistate systems the relation of intensity to population is more complicated than (4), and it will be discussed later.

In the interpretation of the data on NO_2 fluorescence, we have made heavy use of the relations (14-17), (24,25), and (30, 31).

EXPERIMENTAL

An apparatus was designed to excite and detect fluorescence in the visible region and to measure fluorescence lifetimes in the range 10 - 200 μsec at extremely low light intensities. Since it was desired that the excitation band-pass be narrow and continuously tunable throughout the region, a continuum source with double monochromator was employed rather than an atomic line source.

The phase-shift method is especially suitable to lifetime measurements at low fluorescence intensities as it makes efficient use of the available excitation light (50% in the present case) and readily allows for long integration periods necessary to overcome shot noise in the optical signal. Under the con-

ditions of the experiment, at a pressure of 1 mtorr, or 3×10^{13} molecules/cm^3 in the ground state, there were typically 10^3 molecules/cm^3 in the excited state. Signal intensities were of the order of 100 counts/sec; lifetime measurements may be made at intensities well below this (e.g., 10 counts/sec) if the integrating time is sufficiently long for the desired accuracy. The present apparatus measures the fluorescence phase lag as the ratio of the quadrature component of the optical signal to the in-phase component. This technique enables integration times to be extended arbitrarily by analog or digital means.[4,27]

A block diagram of the apparatus is given in Figure 1; the individual components are discussed briefly below. A complete description of the apparatus is given in Ref. 1.

The light source was a 1600 w dc, high pressure xenon arc (Osram model XBO), which emits a continuum from 2400 to 7600 A. According to the manufacturer there is some structure to the emission spectrum of the lamp in the region 4400-5000 A, probably pressure broadened lines; however, no indication of this structure was observed in the output radiation of the source monochromators. The stability of the lamp was normally within ± 2% during the course of an experiment; possible long term drifts in the lamp intensity or detector sensitivity were compensated by the use of a reproducible fluorescence intensity standard. As an additional precaution experiments were conducted in random order.

The exciting light was sent through a double monochromator, Bausch and Lomb 33-86-02 (compact) and 33-86-45 (500 mm) grating monochromators in series. The former, used as a pre-monochromator

to reduce scattered light, was mounted at the side slit of the larger instrument so that the entrance slit of the second monochromator served as the exit slit of the first Under the usual conditions of measurement the slit widths were 1.3 mm for the entrance slit of the compact monochromator and 0.9 mm for the slits of the 500 mm monochromator. At these slit widths the nominal full width at half maximum intensity was 11.5 A. The slit function was observed with a Spex Industries model 1400 double grating monochromator. In order to obtain a representative sampling of the excitation radiation the entire beam was made to fall on a frosted glass plate, and the scattered light from this plate was observed in transmission. The slit function was approximately symmetric. Under the usual conditions the full width at half intensity was 15A; the 10% width was less than 30 A and the 1% width less than 40 A.

The optical modulator was a 60-bladed chopper wheel rotated at 60 revolutions/sec to provide a modulation frequency of 3600 Hz, corresponding to a tuned lifetime (45° phase shift) of 44.21 μsec. The modulation frequency was confirmed by direct count and was considered to be maintained to the precision of the 60 cycle ac line frequency, which is generally better than 0.1%. The width of the blades was equal to that of the slots. The image of the source monochromator exit slit on the blade was approximately 1 MM wide compared to 5.2 mm for the blades. It was desired to have the image of the slit focused as small as practical in order to minimize phase spread in the excitation radiation.

Because of the effect on the measurements of the fluorescence geometry it is desired to keep the observation region large. The geometrical arrangement is shown in Figure 2. The excitation beam B was approximately parallel throughout the cell. The two masks M served to prevent observation of any possible fluorescence by the walls of the cell and to prevent detection of fluorescence from molecules excited near the walls whose lifetime would be shortened by wall quenching. The aperture of the photomultiplier housing was designed not to restrict the observation region. The most severe limitation of the detection efficiency at large distances from the axis was the curvature of the spherical fluorescence cell; at larger angles from the normal a higher fraction of incident light is reflected. Because of this effect the estimated dimension of the region of good detection efficiency was ± 14 cm about the axis.

The optical detector was an EMI 9558A photomultiplier, which has a sensitivity extending to 8000A (S-20 response). The tube was refrigerated by cold N_2 gas passing over the cathode area; the temperature was -56° ± 4° C. Any dependence of the quantum efficiency of the photomultiplier in this temperature range was less than 1%. The dark current was approximately 40 counts/sec. A stabilized high voltage power supply (Fluke model 408B) was used.

The spectral response of the detector (interference filters plus photomultiplier) was calibrated by use of a tungsten ribbon filament lamp (General Electric model 30A/T24/17) whose temperature was determined with a calibrated optical pyrometer. From the brightness temperature the thermodynamic temperature and spectral emissivity were determined from the data of

De Vos[28] with a program written by Gabelnick.[29] The interference filters were obtained from Baird Atomic Corp.

The electronics for handling the signal from the photomultiplier was a hybrid digital-analog circuit similar to that described by Akins, Schwartz, and Moore.[30] In this method each single-event pulse from the photomultiplier triggers a digital circuit to produce an output pulse of constant voltage and duration. This pulse is subsequently handled by analog circuitry, in the present case a Princeton Applied Research Model JB5 lock-in amplifier. The use of analog circuitry allowed for the selection of the fundamental frequency component of the modulated fluorescence signal and for resolution of the fluorescence into in-phase and quadrature components. Because of the single-shot characteristics of the input optical signal it was necessary to operate the lock-in amplifier at a low average dc output voltage in order to avoid saturating ac amplifiers by high transient voltages. A sharply tuned amplifier, such as is in the signal channel of the JB5 lock-in, serves to reduce the required dynamic range of analog photon counters. The output of the lock-in amplifier was integrated digitally by the method of Morris and Johnston.[27]

The reference signal to drive the lock-in was taken directly from the motion of the chopper blade by a metal distance detector (Bently Nevada Corp., Model D-152). This signal is capable of driving the lock-in directly at any given phase; however, since the lock-in used did not have a quadrature phase shifter, such a phase shifter was constructed so that reference signals separated by 90° could be obtained.

The vacuum and gas handling system was a conventional greaseless, mercury-free metal and glass line. High vacuum greaseless stopcocks (Teflon plugs, O-ring seals) were used. The fluorescence cell was a 33 cm diameter, 22 liter pyrex spherical bulb. The neck was sealed against the atmosphere with a 10 mm greaseless stopcock; the leak rate into the sealed-off cell was less than 5×10^{-7} torr/h. Most experiments were made within a period of 10 hours after the cell was filled, but in a few cases measurements were continued on the next day. A cold finger was attached to the cell to allow for freezing out the sample.

Pressure measurements were made with a capacitance pressure transducer (Datametrics models 511-10, 1014). The linearity was stated to exceed 0.1% over the range 0-10 torr; in the present experiment with analog read-out (Varian G-10 recorder) measurements were precise to ± 1%. A finite leak rate in the transducer produced a zero offset in the pressure measurements; consequently measurements were made by difference. The impurity in the sample due to this leak was estimated to be less than 0.03 mtorr; this was probably the most significant source of impurity.

Nitrogen dioxide, obtained from Matheson, had a stated purity of 99.5%. The gas was further purified by crystallization at -78°C followed by pumping and bulb-to-bulb distillations. The crystals were colorless. The purified sample was kept in the dark at -196°. Prior to filling the cell the sample was recrystallized within the storage bulb and again pumped on at -78°. The cell was filled by admitting NO_2 from the storage bulb

at -78° until the desired pressure was attained. The equilibrium with N_2O_4 was of no significance at the pressures used.[31] The experiments were conducted at 23.3 ± 1.3°C.

For any set of independent variables (excitation wavelength, observation wavelength, and pressure) the two measured quantities were the intensities of the in-phase and quadrature fluorescence. In practice, however, some scattered modulated light (source light transmitted through the interference filter) is detected by the photomultiplier; consequently all measurements were made as a difference between signal with the fluorescing gas present and with the gas frozen out. For each of the four measurements usually three to six readings were made of the signal intensity. The length of the integration period and the number of readings made were determined from estimates of the signal-to-noise.

In order to set the phase of the lock-in detector to that of the excitation radiation it was necessary to observe a representative sample of that radiation suitably reduced in intensity. This was accomplished by use of the ground-glass scatter plate and neutral density filters. When the lock-in is correctly phased, the signal for in-phase detection is at a maximum; for quadrature detection, at a minimum. Measurement of the phase error is more sensitive in the quadrature channel; this error was measured as $\Delta\phi = S_{-90}/S_o$. The required tolerance on phase error was 1%. After several fluorescence measurements the phase error was again measured to check for any drift.

RESULTS

A. Effect of Size of Fluorescence Cell

In exploratory investigations it was established that the measured lifetime at low pressures was a function of the size of the fluorescence cell. After the apparatus had been adapted to use with a 33 cm spherical bulb as fluorescence cell, a quantitative measure of this effect was obtained by using cells of different size. Two cylindrical pyrex cells (4.6 cm and 9.6 cm inner diameter) were used in addition to the 33 cm spherical bulb. As with the spherical bulb, the ends of the two cylindrical cells were masked from the view of the photomultiplier. The dimensions are given in Table I. For this experiment the excitation beam was approximately rectangular having dimensions 2.0 x 1.5 cm. All three cells were filled to a pressure of 1.3 ± 0.1 mtorr. Excitation was at 5175 A and detection was with a corning 2-73 filter. The lifetimes, computed under the assumption of a single excited state, are given in Table I.

Table I

Effect of size of fluorescence cell on measured lifetime

Cell Diameter cm	Overall length cm	Length of cell visible to PMT cm	Apparent lifetime μsec
4.6	7.5	3.0	44
9.6	12.5	5.5	68
33, spherical	---	19.8	80

B. Fluorescence Lifetime as a Function of Excitation Wavelength

In this study the fluorescence cell was filled to a low pressure (1.3 ±).1 mtorr) and the fluorescence lifetime was measured for excitation wavelengths from 3975 A to 6000 A. The excitation band-pass was approximately 25 A, full width at half maximum. The fluorescence was observed through a Corning 2-73 filter for excitation wavelengths shorter than 5400 A, or the appropriate "sharp-cut" filter for higher excitation wavelengths. The measured lifetimes were 60-90 μsec throughout the excitation region. The data are given in Figure 3. Figure 3 also shows the results of several individual measurements for excitation in the region around 5175 A with an excitation band-pass of 12 A. The lifetimes were computed on the assumption of a single excited state (10) and were not corrected for quenching. Since an observed lifetime at finite pressure (14) is shorter than the radiative lifetime these measurements represent a lower bound to the radiative lifetime. However at the pressure of these measurements quenching would not shorten the lifetime by more than ten or twenty per cent.

Considerable attention was paid to the possibility that systematic errors might be responsible for observed fluctuations in the measured lifetime. To avoid this possibility measurements of lifetimes at different excitation wavelengths within a narrow region were made in random order, and the phase of the instrument was checked frequently and at different wavelengths.

In addition to low-pressure studies, exploratory investigations were made at a higher pressure (36.0 mtorr) to extend the

range of excitation wavelengths to higher values. The higher pressure was necessitated by the decrease in fluorescence signal in the extended region. At the higher pressure the lifetimes were of course shortened signficantly from the radiative lifetimes by quenching processes. At 36 mtorr, it was possible to measure fluorescence lifetimes for excitation as far to the red as 6800 A. The observed lifetime (due to quenching and fluorescence) was relatively constant as a function of excitation energy for excitation throughout the region, (Figure 3).

C. Pressure Dependence of Fluorescence Lifetime and Intensity

These studies were conducted over the pressure range 0.5 to 50 mtorr for three excitation wavelengths, 4000, 4300 and 4800 A. For each set of experimental conditions (excitation wavelength, observation wavelength, and pressure) the raw data were averaged and appropriate differences taken to correct for scattered light from the empty cell. The quantities thus obtained, S_{0} and S_{-90}, were the uncorrected in-phase and out-of-phase signal intensities. These intensities were normalized by dividing by the pressure of the absorbing gas and corrected for the wavelngth response of the system for the interference filter used. These corrected data were used to compute the linear-mechanism (1, 9) quantities, $\underline{k}$ (7, 9, 10) and $\underline{J}$ (8, 11, 12). For each set of measurements with a given excitation and observation wavelength the quantities $\underline{k}$ and $\underline{J}^{-1}$ were graphed as a function of pressure (14, 15) and fitted by the method of least squares. These quantities were selected to be fitted

because the Stern-Volmer model predicts linearity.

The results of these studies may be briefly summarized. The fluorescence was found not to obey Stern-Volmer (single excited state) kinetics. The measured lifetimes were different at different observation wavelengths. The quantities $\underline{k}$ and $J^{(-1)}$ exhibited pressure dependences that were different from one observation wavelength to another and from one another at the same observation wavelength. Further, the graphs of these quantities as a function of pressure were not, in general, linear. Considered as a function of fluorescence energy the observed lifetimes at high pressures were much shorter at high energies, close to the excitation energy, than at lower energies. That is, the quenching curves were steeper, the smaller the energy difference between excitation and observation. Similarly the fluorescence intensity spectra showed a considerable shift toward lower energy (red shift) as the pressure was increased. These results will be discussed in more detail in the remainder of this section.

We consider first the "lifetime" data. In Figure 4 are given examples of conventional Stern-Volmer plots of such data. The zero-pressure intercepts of these graphs should, in the single-state assumption, correspond to the fluorescence rate constants (inverse radiative lifetimes). If an observed state is excited both directly and by a pressure dependent cascade process, the zero pressure intercept should nevertheless be the fluorescence rate constant for the state. However, there is a significant amount of variation in these zero pressure intercepts (for a given excitation wavelength) indicating that

molecular states of considerably different lifetimes are directly populated by the excitation light within the band-pass of the monochromator. Since the observations yield an average of the detected fluorescence rates, the observed variation, which was as great as 30%, sets a lower limit to the variation in the rate constants of the individual quantum states.

For observation energies close to the excitation energy plots of $\omega/\underline{R}$ vs. M were linear. Interpreted in terms of the Stern-Volmer mechanism (14) the slope of such a graph is a quenching rate constant. Values for rate constants obtained in this way are given in Table II. From fitted functions for ω/R as a function of M at the several observation energies, the Stern-Volmer lifetimes at various pressures were computed and plotted as a function of fluorescence energy (Fig. 5). The points were connected by interpolation, which is given as merely suggestive.

Table II

Apparent quenching rate constants for fluorescence at energy close to energy of excitation

Energy of excitation A	Energy of excitation cm^{-1}	Energy of observation cm^{-1}	q_{sv} cm^3/molecule sec	P
4000	25000	23200	1.92×10^{-10}	0.84
4300	23260	22170	1.26×10^{-10}	0.55
4800	20830	19960	1.60×10^{-10}	0.70

Quenching rate constants were computed from slopes of Stern-Volmer lifetime graphs. P is "quenching" probability per gas kinetic collision, computed using molecular diameter from Ref. 32. q_{sv} is the Stern-Volmer quenching constant.

The lifetime data were also plotted according to the inverse Stern-Volmer relation (16). A finite, non-zero intercept in such a plot indicated that there is a first order dependence of the inverse lieftime upon pressure at the high pressure limit; this was found to be the case in all instances. Spectra of the infinite pressure limit of the lifetimes, $\underline{Q}^{-1}$ (24), are given in Figure 5.

The intensity data were graphed according to the Stern-Volmer theory in the same way as the lifetime data. These data exhibited finite intercepts in both the conventional and inverse plots. As with the lifetime data, the intensities from the fitted functions were graphed as a function of fluorescence energy (Figure 6). In these graphs (for the first time in the presentation of the data) the relative response factors of the detector for the various interference filters have been employed; any error in the determination of these response factors will enter into the intensity spectra as the systematic raising or lowering (by a fixed amount) of the intensity at one observation energy relative to that at another. Again, from the high pressure slopes of the data it was possible to calculate infinite pressure limits, $\underline{Y}$ (25), to the intensity spectra. These data are given in Figure 6.

It should be pointed out here that the fluorescence spectra extended in all cases beyond the limit of observation (7000 or 8000 A). This was true for the resonance fluorescence (zero pressure) spectra as well as those at higher pressures, indicating that a broad spectrum is a property of molecules within

a localized energy region and not merely the consequence of a broad distribution function of molecular energies.

DISCUSSION

A. Effect of Molecular Migrations on Lifetime Measurements.

The low pressure lifetimes obtained in the present experiment (55-90 μsec) are significantly longer than have been reported previously by Neuberger and Duncan[5] and by Douglas[7] (44 μsec). It is believed that the longer lifetimes measured are due to the use of a fluorescence cell of sufficiently large diameter that the measured lifetime is not governed by wall collisions, or by collision-free migration of excited molecules outside the region of observation. This interpretation is based on the following considerations:

1) A calculation was made of the effect of molecular migration on measured lifetimes and quantum yields of fluorescence. The calculation was based on the assumptions of the Maxwell-Boltzman velocity distribution and exponential decay, and was performed for cylindrical geometry with excitation taking place along an infinitely narrow line. The results are given in Figure 7, as a function of the radius of observation measured in units of the product of the lifetime times the most probable velocity. For NO_2 at 295° K, assuming a lifetime of 80 μsec, this distance, $\underline{r}$, is 2.7 cm. The radius of observation used in the present experiment was 14 cm or $5\underline{r}$. Thus the error in the lifetime from molecules leaving the region of observation would be no more than a few percent. The previous investigators

did not state the dimensions of their fluorescence geometry, so that a direct evaluation from Figure 7 of possible shortening of their measured lifetimes is not possible.

2) The measurements of fluorescence lifetimes made with cells of smaller dimensions were significantly reduced from the lifetimes with the 33 cm cell and were consistent with the predictions of Figure 7. This may be taken as direct evidence of the effect of molecular migration of the order of 5 cm and of quenching upon collisions of excited molecules with the walls of the cell.

3) The measured lifetimes in the 33 cm cell showed a significant (50%) dependence upon the excitation wavelength; such a dependence was not observed previously.[5] While the existence of such a dependence does not demonstrate that the dimensions of the observation region have been extended sufficiently, it does suggest that the measured lifetimes are at least approaching the true values.

B. The Radiative Lifetime of NO_2 ($^2B_1$) and Low-pressure Data

The extension of the Einstein relation between the absorption coefficient and the radiative rate constant to molecular transitions, under the assumptions of the Born-Oppenheimer approximation and of a constant electronic transition moment, was made by Mulliken.[33] The applicability of this relation has been extended by Strickler and Berg,[8] who have explicitly considered the effect of any shift in the fluorescence energy from that of absorption. The Einstein relation as applied to molecular transitions may be written

$$A = 8\pi c \frac{g''}{g'} \langle \tilde{\nu}^3 \rangle_{F\text{-}C} \int \frac{\sigma(\tilde{\nu})}{\tilde{\nu}} d\tilde{\nu} \qquad (32)$$

where A is the radiative rate constant;

g' and g'' are respectively the numbers of levels in the upper and lower states to which transitions can take place;

σ is the absorption coefficient in units cm^2; the integration is to be performed over the entire elctronic absorption spectrum; and

$\langle \tilde{\nu}^3 \rangle$ is the Franck-Condon average of the emission energy-cubed,

$$\int I_{\tilde{\nu}} d\tilde{\nu} \Big/ \int \frac{I_{\tilde{\nu}}}{\tilde{\nu}^3} d\tilde{\nu}$$

Here $I_{\tilde{\nu}}$ is the emission intensity (quanta/cm^{-1} sec) and the integrations are to be performed over the emission spectrum. The quantity $\langle \tilde{\nu}^3 \rangle_{F\text{-}C}$ might be expected to depend on the vibrational level of the upper state, and consequently the lifetime as well, with more highly energetic states expected to have a shorter lifetime.

For application of the radiation relation to predict the lifetime of a molecule in any given quantum state not only the absorption spectrum, but also the emission spectrum of that particular state must be measured. The entire resonance fluorescence spectrum of any vibrational level of NO_2 has never been measured; consequently the value of the average quantity $\langle \tilde{\nu}^3 \rangle_{F\text{-}C}$ is not known. However this quantity may be estimated

by various means. First, from the absorption spectrum the average frequency of absorption may be determined[5] (Table III) and used as an estimate of the fluorescence frequency. However this quantity would be expected to be too large because, while absorption continues well beyond the predissociation limit[9] fluorescence is entirely at lower energies,[5,35] and because much fluorescence takes place to high vibrational levels of the ground state, with a reduction in the ν'^3 factor. A second approach to the value of $\langle \nu'^3 \rangle_{F-C}$ can be made through the use of the luminescence spectra of chemical reactions that yield excited NO_2, if it may be assumed that the electronic state here is the same as that populated optically. Values obtained from the NO + O and NO + O_3 spectra are given as well in Table III. The two values given might be taken to represent the average fluorescence energy for the two molecular energies populated by the reactions; however, since the spectra are obtained at high pressure, energy transfer processes will have taken place, and consequently the spectra are shifted to lower energies than the resonance spectra. Thus the values obtained should only be considered as rough estimates of the $\langle \nu'^3 \rangle_{F-C}$ factor to be used in applying the radiation relation. Certainly the spread in the values obtained for $\langle \nu'^3 \rangle_{F-C}$ indicates the degree of caution that must be exercised in applying this relation to a transition that extends over as wide a region as the present one.

The results of the present measurements were at variance from the predictions in several ways:

1) The absolute magnitudes of the fluorescence lifetimes

Table III

Fluorescence lifetime of NO_2 calculated from radiation relations

Integrated Quantity	Value	Calc. Lifetime, μsec	Source of Data	Ref.
$\int (\sigma/\tilde{\nu})\, d\tilde{\nu}$	2.99×10^{-19} cm^2		absorption	34,35
$\int \sigma d\tilde{\nu} / \int (\sigma/\tilde{\nu})\, d\tilde{\nu}$	25880 cm^{-1}	0.256	absorption	34,35
$[< \tilde{\nu}^3 >_{F-C}]^{1/3}$	12300 cm^{-1}	0.38	NO + O	13,36
$[< \tilde{\nu}^3 >_{F-C}]^{1/3}$	6233 cm^{-1}	18.3	NO + O_3	14,15

Results of numerical integrations of absorption and fluorescence spectra. Fluorescence lifetimes were calculated from integrated absorption coefficient, $\int (\sigma/\tilde{\nu})\, d\tilde{\nu}$, using three estimates of the mean frequency of fluorescence.

were greater than predicted by a factor of 3 to 40, depending on the value of $\langle \tilde{\nu}^3 \rangle_{F-C}$ used.

2) The ratio in observed lifetimes at the extremes of excitation energies used (4000 to 6000 A) was only 1.6, whereas, other things being equal, the energy difference would lead to a prediction closer to $(6000/4000)^3 \simeq 3.4$.

3) Distinct fluctuations were observed in the radiative lifetimes as a function of excitation energy and also for the narrow spread in excitation energy in the monochromator band pass (60 cm^{-1} full width at half maximum).

The inadequacies of the simple radiation relation may be considered in terms of the two assumptions upon which it was based, namely the Born-Oppenheimer approximation and the assumption that the transition moment is constant for the molecular geometries involved in the transition.

The possible dependence of the transition moment on the molecular geometry has been propsed by Mulliken[37] as a cause of the anomalously long lifetime of NO_2. From molecular orbital correlation diagrams[18] it is expected that the $^2B_1$ state of NO_2 would be more nearly linear than the ground state, and this expectation has been confirmed by the analysis of the absorption spectrum.[9] Thus a decrease in the transition moment as the molecule becomes more nearly linear would be expected to increase the radiative lifetime. However, if such a mechanism were responsible for the long lifetime, the lifetime would be expected to decrease rather strongly with increasing quantum number in the bending vibration, and correspondingly with the energy of

the upper state. Since the observed low-pressure lifetimes were more constant as a function of excitation energy than expected, this mechanism does not appear to be the reason for the increased radiative lifetime.

Jortner and coworkers have recently considered the validity of the Born-Oppenheimer approximation in molecular transitions.[38-40] If there exist perturbations between the upper electronic state and any other electronic state having an appreciable level density in the absorption region, then the Born-Oppenheimer wave functions will not adequately describe the upper state. Under these circumstances the transition moment to the ground state of a single Born-Oppenheimer vibronic level will be distributed among several true vibronic levels, the number of which is determined by the density of the manifold of states which are not connected to the ground state in the Born-Oppenheimer approximation. The total transition moment, as measured by the absorption coefficient integrated over the electronic transition, is conserved; however, the transition moment to the ground state from a given true vibronic level, which determines the radiative lifetime, is reduced by the factor $|\langle \psi_{true} | \psi_{B-O} \rangle|^2$.

For NO_2 the Renner effect is a possible mechanism which is available to connect the levels of the $^2B_1$ state with the dense manifold of high vibrational levels of the ground state.[9] A consequence of the perturbative mechanism of lengthening the lifetime would be the possibility of significant fluctuations in the molecular lifetime within a narrow energy region.[7] Such fluctuations have been observed in the present experiment. A mechanism based on the Renner effect coupling would require

that levels which are, for symmetry reasons, unperturbed exhibit much shorter lifetimes than the perturbed levels. However, in an experiment such as the present one such short lived states would contribute to the total fluorescent intensity only in proportion to their absorption, and would not be detected in the presence of a much greater signal from states having a long lifetime. If such short lived states contributed significantly to the total signal intensity, their presence would lead to Stern-Volmer plots whose (positive) slope decreased with pressure; no such behavior was observed.

Related to the theory of intra-molecular lengthening of lifetimes that has been outlined is an inter-molecular process that has been proposed by Jortner and Berry.[39] The dense manifold of states which are not optically connected to the ground state is collisionally populated at finite pressures, and the apparent lifetime of fluorescence is consequently lengthened. Jortner and Berry do not indicate the magnitudes of collision cross-sections that might be expected for this type of process. However, such a mechanism would imply that, at sufficiently low pressures, the fluorescence lifetime would be short. The question is thus raised whether the present experiments have been conducted at pressures sufficiently low to observe resonance fluorescence and to allow a confident extrapolation to zero pressure. This question is, of course, open to further experimentation either at lower pressures or in collision-free molecular beams. However, we should like to point out that the present measurements were performed at pressures such that the average molecule at the assumed long lifetime suffered as few

as 0.2 gas kinetic collisions; if the "resonant" lifetime were significantly shorter than 60 μsec, the number of collisions of the average molecule would be correspondingly reduced. In no case , for either intensity or lifetime data, was there any indication of a discontinuity in the pressure dependence of the data which would cause us to question the extrapolation to the limit of zero pressure.

C. Interpretation of High-Pressure Data

The observed limiting high-pressure quenching constants $\underline{Q}$ (24) and the high-pressure fluorescence intensities $\underline{Y}$ (25) are listed in Table IV for each observation energy $\underline{W}$. The observations for excitation at 25000 cm^{-1} are more extensive than those at other excitation energies; and for these data the relative reciprocal quenching constants $\underline{Q}^{-1}$, are listed in Table IV. As can be seen from Figure 6a the intensity at zero pressure is roughly (overlooking what appears to be some real structure) the same at all frequencies between 12500 cm^{-1} and 24000 cm^{-1}, even though all molecules were at the excitation energy, 25000 cm^{-1}. The actual fluorescence at energy $\underline{W}$ is given not only by molecules with energy $\underline{W}$ but also by all molecules with energy greater than $\underline{W}$. Thus the population (31) is more nearly given by the derivative of the intensity (25) with respect to energy rather than to the intensity itself

$$\underline{P}\ (\underline{W}) = d\ \underline{Y}\ (\underline{W}) \ /\ d\ \underline{W} \qquad (33)$$

The intensity data $\underline{Y}$ of Table IV at 25000 cm^{-1} were found to vary as $(\underline{W}_x - \underline{W})^{1.30}$, and thus the population $\underline{P}$ varies as

$(W_x - W)^{0.30}$, which is entered as the last column in Table IV. The overlapping of the fluorescence spectra from different energy states has less effect on the observed Q^{-1} than on the intensities, since both the population and Q^{-1} increase with decreasing energy. Even so, the relative Q^{-1} as a function of molecular energy must increase with decreasing energy somewhat more strongly than given in Table IV.

The high-pressure data are interpreted in terms of RRK stepladder[25,26] models (26), one for the excited electronic state E and a similar one for the ground electronic state G. The three normal-mode vibrational frequencies[41] of G are 1320, 750, and 1618 cm^{-1}; and the convenient round-number 1250 cm^{-1} is very close to the average. Thus the RRK model of G is

$$s = 3$$
$$\epsilon = 1250\ cm^{-1} \qquad (34)$$

epsilon

where ϵ is the level spacing and s is the number of normal modes. The molecule dissociates at 25000 cm^{-1}, so this model has 0 ⋯ 20 energy levels with multiplicity given by (26).

The properties of the upper electronic species E are not precisely known. The observed fluorescence may involve one or more electronic states. The excited molecule may be linear ($s = 4$) or bent ($s = 3$). The origin of the upper state has been placed[9] between 11500 and 15500 cm^{-1}. For purposes of model calculations we assume the excited species to be a single electronic state with the properties

$$\underline{s} = 3$$
$$\epsilon = 1250 \text{ cm}^{-1}$$
$$\text{origin above origin of } G = 12{,}500 \text{ cm}^{-1} \tag{35}$$

Between 12500 and 25000 cm^{-1} there are eleven energy levels, 0 ... 10.

The reciprocal quenching constant $\underline{Q}^{-1}$ (24) may be regarded as an observed (Table IV), continuous function of energy $\underline{W}$. From the stepladder model (30) the slope of the reciprocal quenching constant vs energy is simply

$$\frac{d\,\underline{Q}^{-1}}{d\,\underline{W}} \; \frac{d\,\underline{W}}{d\,\underline{n}} = \frac{1}{\underline{q}\,(\underline{w}) + \underline{b}\,(\underline{w})} \tag{36}$$

where $d\,\underline{W} / d\,\underline{n}$ is the energy removed per collision for which the total quenching constatn is $\underline{q} + \underline{b}$. Although the Stern-Volmer plots are curved when observed over a wide range of pressure (especially for observation energies $\underline{W}$ far removed from the excitation energy $\underline{W}_x$), these plots are very nearly linear over a moderate range of pressure when $\underline{W}$ is close to $\underline{W}_x$. Thus for a narrow range of energy just below the excitation energy a Stern-Volmer plot gives the total quenching constant, $\underline{q} + \underline{b}$, (Table II). A separate plot of $\underline{Q}^{-1}$ vs $\underline{W}$ gives the slope $d\,\underline{Q}^{-1}/d\,\underline{W}$; and from (36) we may calculate the average energy removed per collision $d\,\underline{W}/d\,\underline{n}$ for energies close to the excitation energy. The results of these computations are given in Table V. The magnitude of column (b) indicates a very great

rate of fluorescence quenching. Using the Stern-Volmer quenching constants from Table II, we find that the energy removed per collision is very large, between 2000 and 4000 cm^{-1} are indicated. Alternatively, using the RRK model where the energy removed per collision is taken to be 1250 cm^{-1}, the total quenching constant is about 4×10^{-10} cc/particle-sec, almost twice the hard-spheres collision constant for NO_2, 2.28×10^{-10} cc / particle-sec. Thus the separate results of Table II and Table V indicate that per hard-spheres collision, highly vibrationally excited NO_2 are de-activated the order-of-magnitude of a thousand wave numbers. Thus to complete the step-ladder model as given by (35), we identify the ladder spacing ϵ with the energy removed per collision (36)

$$\epsilon = d\underline{W} \,/\, d\underline{n} \;=\; 1250 \text{ cm}^{-1} \qquad (37)$$

Table IV

Observed high pressure limiting quenching constants (24) and intensities (25)

	10^{11} Q, cc/sec			Relative Y			Relative Q^{-1}	Relative P
W exc.	25000	23256	20833	25000	23256	20833	25000	25000
W cm^{-1} abs								
25000							1.00	1.00
23200	19.2			.72			2.74	1.19
22170	13.0	12.6		1.02	2.60		4.05	1.37
21460	11.7			1.82			4.50	1.46
20790	9.39	9.49		2.20	7.87		5.61	1.54
20370	8.63			2.35			6.11	1.58
19960	8.20	9.51	16.0	3.08	11.8	4.29	6.42	1.62
19350	7.95	8.74	11.6	3.38	14.1	5.21	6.61	1.68
18950		7.34			15.9			
17880	6.49	6.87	9.64	4.75	21.3	9.70	8.10	1.80
16960	5.64	6.06	8.11	5.89	28.6	17.9	9.35	1.87
15850	5.06	5.29	6.69	5.44	29.4	18.5	10.4	1.94
15130	4.46	4.70	6.06	5.32	30.6	19.2	11.8	1.99
14270	4.12	4.31	5.47	6.06	35.6	25.6	12.8	2.03
13320	3.83			10.2			13.7	2.09
12480	3.70			8.27			14.2	2.13

Table V

Quantities derived from fluorescence observed close to excitation energy

$\frac{W}{7}x$	$\frac{d\,Q^{-1}}{d\,W}$	$(q + b)$	$\frac{d\,W}{d\,n}$	$(q + b)$
(a)	(b)	(c)	(d)	(e)
25000	4.8×10^{-7}	1.9×10^{-10}	2500	3.9×10^{-10}
23260	5.1×10^{-7}	1.3×10^{-10}	4000	4.1×10^{-10}
20830	4.9×10^{-7}	1.6×10^{-10}	3000	3.9×10^{-10}

(a) Excitation energy, cm^{-1}.

(b) Q^{-1} in units of particle-sec/cc and W in cm^{-1}

(c) Total quenching constant from limited Stern-Volmer plot, Table II; units of cc/particle-sec.

(d) Energy removed per collision, cm^{-1}, calculated from (b), (c) and (36).

(e) From (b) and (36) where d W/ d n is taken to be 1250 cm^{-1}.

Consider a set of three adjacent, decreasing, vibrational energy levels, $j + 1$, j, and $j - 1$ with multiplicities g_{j+1}, g_j, and g_{j-1}.

$$E_{j+1} \xrightarrow{b_{j+1}^M} E_j \xrightarrow{b_j^M} E_{j-1} \tag{38}$$

The relative rate of vibrational deactivation is given by the product of an appropriate transition moment times the multiplicity of the final state.[42] For highly excited vibrational states, the transition moments may vary slowly with energy, leaving the multiplicity factors as the dominant term. It is reasonable to assume that the vibrational quenching constants between successive energy levels vary as the multiplicity of the final state

$$\frac{b_{j+1}}{b_j} \approx \frac{g_j}{g_{j-1}} \tag{39}$$

Thus except for an undetermined constant, the set of vibrational quenching constants, b_j, can be calculated from (26) and (39).

The electronic quenching constants, q_j, refer to the physical act of collisional transfer from the j vibrational level of E to any vibrational state of G. For these model calculations it is assumed that the electronic quenching constant is the same for all vibrational states, that is, $q_j = q$, a constant. Various values of q, relative to the vibrational quenching constant of the top vibrational state, b_p, are assumed. In this way all parameters are fixed to calculate the

relative reciprocal quenching constants $\underline{Q}^{-1}$ (30) and the relative populations $\underline{P}$ (31) for a direct comparison with the experimental quantities.

Based on the model developed above for the ground electronic state G and the excited electronic state E, the vibrational energy level $\underline{j}$, the multiplicity $\underline{g}_j$, the relative reciprocal quenching constant $\underline{Q}^{-1}$, and the relative population $\underline{P}$ are listed in Table VI for the special case of $\underline{q} = 0$. For the excited state E, various values of the electronic quenching constant between $\underline{q} = 0.075\ \underline{b}_{10}$ and $q = 0.30\ \underline{b}_{10}$ were assumed, and the terms $\underline{Q}^{-1}$ and $\underline{P}$ were calculated and plotted in Figure 8, which also shows the experimental points from Table IV. The observed reciprocal quenching constants $\underline{Q}^{-1}$ vary much more slowly with energy than the calculated ones for $\underline{q} = 0$. The calculated $\underline{Q}^{-1}$ curve is brounght closer to the observed $\underline{Q}^{-1}$ points if large values of the electronic quenching constant are assumed. However, the relative population is an extremely sensitive function of the assumed value of $\underline{q}$. For all excitation wavelengths the population inferred from the fluorescence increases with decreasing energy over the entire range of observations. As can be seen from (31), this result implies the following inequality for all j

$$\underline{b}_{j+1} > (\underline{b}_j + \underline{q}) \qquad (40)$$

To satisfy (40) at all energies above 14000 cm^{-1}, $\underline{q}$ cannot be greater than $0.05\ \underline{b}_{10}$. With a value of $\underline{q}$ equal to or less than $0.05\ \underline{b}_{10}$, there is very poor agreement between calculated and

observed reciprocal quenching constants. Thus the step-ladder model for the excited state E (35, 37) fails to agree with the experimental data, and any adjustment of parameters designed to improve the fit to the reciprocal quenching constants gives totally false predictions for the populations.

These calculations were applied to the top vibrational levels of the ground electronic state G. With the assumption that the electronic quenching constant $\underline{q}$ is zero, the calculated curves for $\underline{Q}^{-1}$ and $\underline{P}$ are given in Figure 9. In this case there is excellent (in view of the simplicity of the model) agreement between calculated and observed quantities for both the reciprocal quenching constants and the relative populations. Thus these experimental data on high-pressure quenching kinetics indicate that optical excitation and fluorescence occur to and from the excited electronic state E, but vibrational deactivation occurs primarily in the high vibrational levels of the ground electronic state G. This result implies a rapid, spontaneous interchange at constant total energy between high vibrational states of E and very high vibrational states of G. In this situation the collision induced transfer from E to G loses its significance as "electronic quenching," and it is appropriate that $\underline{q}$ be zero.

To explain the anomalously long radiative lifetime of excited NO_2, it has been proposed[43] that E and G states interchange with each other at constant energy. Since the G state has a higher multiplicity than the E state, the molecules would spend a correspondingly longer time in the G state. The radia-

tive excitation and fluorescence of the E state is modified by the side-trip of the energetic molecule into very high vibrational levels of G. (This pictorial, kinetic description is more properly expressed in terms of perturbed excited states similar to the situation in predissociation as described by Robert Harris.[44] Such a description has been worked out by Jortner and coworkers.[38-40])

These model calculations do not pretend to be the true theoretical analysis of these data. Rather they show that the small decrease in quenching constant[45] over the interval 25000 to 12500 cm^{-1} together with the large increase in intensity is inconsistent with an assumption that the vibrational quenching occurs in the E state. These kinetic data strongly support the proposal that there is an interchange or a perturbation between the states of E and states of G at the same total energy.

Table VI

Fluorescence quantities calculated from RRK step-ladder model

Excited electronic state E					Ground electronic state G			
			Relative				Relative	
W cm^{-1}	j	g_j	Q	P	j	g_j	Q	P
			(a)	(b)			(a)	(b)
25000	10	66	1.00	1.00	20	231	1.00	1.00
23750	9	55	2.20	1.20	19	210	2.10	1.10
22500	8	45	3.66	1.47	18	190	3.32	1.21
21250	7	36	5.50	1.83	17	171	4.67	1.35
20000	6	28	7.85	2.36	16	153	6.18	1.51
18750	5	21	11.0	3.15	15	136	7.88	1.70
17500	4	15	15.4	4.40	14	120	9.80	1.93
16250	3	10	22.0	6.60	13	105	12.0	2.20
15000	2	6	33.0	11.0	12	91	14.5	2.54
13750	1	3	55.0	22.0	11	78	17.5	2.96
12500	0	1	121	66.0	10	66	21.0	3.50

a. The value of q is assumed to be zero; based on (30).

b. Based on (31); $q = 0$.

The results of these energy transfer studies are consistent with those of similar fluorescence studies of large polyatomic molecules,[2] namely that energy transfer cross-sections are comparable to gas kinetic and that large amounts of energy (several hundred or more wavenumbers) are transferred per collision. The present results are also consistent with the interpretations of energy transfer which have been made from chemical activation studies by Rabinovitch and coworkers,[25] in which, again, the occurrence of highly probable, highly efficient collisions by strongly excited polyatomic molecules has been demonstrated.

For highly excited diatomic molecules, fluorescence studies have shown that the efficiencies are rather small, although the cross-sections are large. In a study of I_2 fluorescence Steinfeld and Klemperer[3] have found probabilities per collsion of single quantum transitions (80 cm^{-1}) equal to 0.2; the probabilities for multi-quantum transitions were further reduced. Thus it would appear that NO_2 should be characterized as similar to large polyatomic molecules in its behavior with respect to energy transfer processes, rather than to diatomic molecules.

D. Relation to Other Work:

Since this work was completed we have learned of two other studies of NO_2 fluorescence. In a preliminary note Keyser, et. al.[46] report a radiative lifetime of 55 μsec for excitation at 4358, 5461, and 5780 A. These authors have interpreted d.c. quenching studies in terms of an energy transfer mechanism

similar to the step-ladder model used here. The value obtained for the collisional efficiency was 900 ± 300 cm^{-1}, in reasonable agreement with the present results, considering the approximations of the two analyses.

Sakurai and Broida[47] have studied NO_2 fluorescence excited by several laser lines in the region 4579-5208 A. The fluorescence spectrum from such a narrow excitation source consists of sharp lines superimposed upon a continuum. If it is assumed that the individual quantum states populated by the excitation have radiative lifetimes similar to those measured in the present work, then Sakurai and Broida's data for the quenching of the discrete fluorescence may be interpreted to yield de-population cross-sections which are approximately gas kinetic. The continuum radiation is quenched considerably less strongly than the discrete radiation; this continuum emission is considered to arise from collisional energy transfer from the initially populated states. The decrease in the observed Stern-Volmer constant, which is dependent on the observation energy, may be understood in terms of the stepwise de-excitation model.

In connection with these investigations we wish to stress an important advantage of a.c. quenching studies over d.c. studies. Steady-state experiments are capable of yielding kinetic information only as the ratio of slope to intercept in a Stern-Volmer plot. When the mechanism of fluorescence is more complex than the simple Stern-Volmer mechanism, then the slope may not be constant, although it does reach a constant

high-pressure limit. However, any kinetic information derived from the ratio of this limiting slope to the zero pressure intercept necessarily mixes high and low pressure data. At the two extremes of pressure the relaxation mechanism is entirely different, and, in a low resolution experiment, different quantum states are responsible for the radiation at a given observation wavelength. Thus, any differences in the radiative lifetimes or fluorescence spectra will enter in an unknown way into the kinetic analysis. In a.c. studies kinetic information may be obtained at any pressure, in particular, at high pressures, where the relative populations are constant, apparent quenching constants may be determined without reference to the low-pressure fluorescence, and consequently free of the additional ambiguities associated with a change in the emitting species.

ACKNOWLEDGMENTS

One of us (S.E.S.) is grateful to the National Science Foundation for a Graduate Fellowship. This work was conducted under the auspices of the Atomic Energy Commission.

TITLES TO FIGURES

1. Block diagram of apparatus for phase-shift measurements at low light intensity.

2. Fluorescence geometry: front and side views of geometrical arrangement for excitation and observation of fluorescence. A, aperture plate, 34 mm. diameter. The aperture plate defined an angle of acceptance θ ($\tan \theta = 0.31$) such that all light entrant upon the aperture plate within this angle was detected with equal efficiency; B, excitation beam, 20 mm x 25 mm; C, fluorescence cell, 33 cm diameter; M, masks.

3. Fluorescence lifetime of NO_2 as a function of excitation wavelength, computed under the single-state assumption. Closed circles, 1.3 mtorr; open circle, 36 mtorr. Half width of excitation light was approximately 25A. Error bars are typical and were determined from the scatter of several measurements. Inset shows individual data points for the region around 5175 A excited with 12 A half width. Data points for the same run connected, points within a run were taken in random order.

4. Stern-Volmer graphs of lifetime data. Excitation energy 4800 A or 20830 cm^{-1}. Observation energy: A, 19960; B, 17880; C, 14270 cm^{-1}.

5. a. Excitation energy 4000 A or 25000 cm^{-1}
   b. Excitation energy 4300 A or 23260 cm^{-1}
   c. Excitation energy 4800 A or 20830 cm^{-1}

Lifetime spectra as a function of pressure. Lifetimes, $\omega^{-1}R$, were interpolated at even pressures (the running index in mtorr) and extrapolated to zero and infinite pressure from the Stern-Volmer plots. The relative lifetime distribution obtained from the infinite pressure extrapolation is not scaled with respect to the ordinate.

6. a. Excitation energy 4000 A or 25000 cm^{-1}

b. Excitation energy 4300 A or 23260 cm^{-1}

c. Excitation energy 4800 A or 20830 cm^{-1}

Intensity spectra as a function of pressure. Intensities were computed from fitted curves of I^{-1} (8). The running index gives the pressure in mtorr. The spectral distribution obtained from the infinite pressure extrapolation is not scaled with respect to the ordinate.

7. Radial distribution of fluorescence intensity and lifetime in cylindrical geometry. R is a dimensionless radius equal to the radius of observation (measured from a line source) divided by the product of the lifetime times the most probable velocity. Curve I gives the distribution of fluorescence intensity. The integration over 2π azimuthal distribution of velocities has been included in the evaluation of I. Curve F gives the error in measured quantum made only yield if measurements are madronly of fluorescence originating in the cylindrical volume extending to R. Curve E gives the corresponding error in the lifetime.

8. Interpretation of high-pressure data in terms of the excited electronic species E. Quenching constants calculated according

to (30), for various assumed values of the electronic quenching constant q, and with relative vibrational deactivation constants calculated from (39) and (26). Relative populations are calculated from (31), and observed populations are inferred from observed intensities according to (33). Observed data are from Table IV.

9. Interpretation of high-pressure data in terms of highly vibrationally excited ground electronic state G. Calculations made as in Figure 8.

REFERENCES

1) Based on the dissertation of S.E. S. submitted to the University of California in partial satisfaction of the requirements for the Ph.D. degree; University of California Lawrence Radiation Laboratory Report UCRL-18431 (1968). A preliminary report of this work was presented at the 155th National Meeting, Amer. Chem. Soc., April, 1968.

2) See, for example, B. Stevens, Collisonal Activation in Gases, (Pergamon Press, Oxford, 1967).

3) J.I. Steinfeld and W. Klemperer, J. Chem. Phys., 42, 3475 (1965).

4) J.T. Yardley and C.B. Moore, Jr., J. Chem. Phys., 45, 1066 (1967).

5) D. Neuberger and A.B.F. Duncan, J. Chem. Phys., 22, 1693 (1954).

6) G.M. Myers, D.M. Silver, and F. Kaufman, J. Chem. Phys., 44, 718 (1966).

7) A.E. Douglas, J. Chem. Phys., 45, 1007 (1966).

8) S.J. Strickler and R.A. Berg, J. Chem. Phys., 37, 814 (1962).

9) A.E. Douglas and K.P. Huber, Can. J. Phys., 43, 74 (1965).

10) N. Jonathan and R. Petty, Trans. Faraday Soc., 64, 1240 (1968).

11) K.M. Becker, W. Groth, and F. Jov, Ber. Bunsenges, 72, 157 (1968).

12) A. McKenzie and B.A. Thrush, Chem. Phys. Lett., 1, 681 (1968).

13) A. Fontijn, C.B. Meyer and H.J. Schiff, J. Chem. Phys., 40, 64 (1964).

14) P.N. Clough and B.A. Thrush, Chem. Comm., 1966, 783.

15) P.N. Clough and B.A. Thrush, Trans. Faraday Soc., 63, 915 (1967).

16) M. Nicolet, J. Geophys. Res., 70, 691 (1967).

17) C.A. Barth, Nitrogen and Oxygen Atomic Reactions in the Chemosphere in Chemical Reactions in the Upper and Lower Atmosphere, (Interscience, New York, 1961).

18) A.D. Walsh, J. Chem. Soc., 1953, 2260.

19) A.M. Bonch-Bruevich, Izv. Akad. Nauk. SSSR Ser. Fiz. 20, 591 (1956).

20). H.G. Kloss and G. Wendel, Z. Naturforsch., 16a, 61 (1961).

21) H.S. Johnston, G.E. McGraw, T.T. Paukert, L.W. Richards, and J. Van den Bogaerde, Proc. Nath. Acad. Sci. U.S., 57, 1146 (1967).

22) O. Stern and M. Volmer, Physik z., 20g 183 (1919).

23) A.C.G. Mitchell and M.W. Zemansky, Resonance Radiation and Excited Atoms, (Cambridge Univ. Press, Cambridge, 1961).

24) R.G. Gordon, J. Chem. Phys., 46, 4399 (1967).

25) F.J. Fletcher, R.S. Rabinovitch, H.W. Watkins and D.J. Locker, J. Phys. Chem., 70, 2873 (1966) and references cited to earlier work.

26) L.S. Kassel, Kinetics of Homogeneous Gas Reactions (The Chemical Catalog Co., Inc., New York, 1932).

27) E.D. Morris, Jr. and H.S. Johnston, Rev. Sci. Inst., 39, 620 (1968).

28) J.C. De Vos, Physica, 20, 690 (1954); G.A.W. Rutgers and J. C. De Vos, Physica, 20, 715 (1954).

29) S.D. Gabelnick, Ph.D. Thesis, University of California, Berkeley; to be submitted, 1968.

30) D.L. Akins, S.E. Schwartz, and C.B. Moore, Rev. Sci. Instr., 39, 715 (1968).

31) F.H. Verhoek and F. Daniels, J. Am. Chem. Soc., 53, 1250 (1931).

32) A.K. Barua and T.K. Rai Dastidar, J. Chem. Phys., 43, 4140 (1965).

33) R.S. Mulliken, J. Chem. Phys., 7, 14 (1939).

34) T.C. Hall and F.E. Blacet, J. Chem. Phys., 20, 1745 (1952).

35) J.H. Dixon, J. Chem. Phys., 8, 157 (1940).

36) H.P. Broida, H.I. Schiff, and T.M. Sugden, Trans Faraday Soc., 57, 259 (1961).

37) R.S. Mulliken, Can J. Chem., 36, 10 (1958).

38) M. Bixon and J. Jortner, J. Chem. Phys., 48, 715 (1968).

39) J. Jortner and S. Berry, J. Chem. Phys., 48, 2757 (1968).

40) D.P. Chock, J. Jortner, and S.A. Rice, J. Chem Phys., 49, 610 (1968). We wish to thank Professor Rice for making copies of this and the two preceding references available prior to publication.

41) E.T. Arakawa and A.H. Nielson, J. Mol. Spectr., 2, 413 (1958).

42) A. Messiah, Quantum Mechanics, (John Wiley and Sons, Inc., New York, 1966). p. 836.

43) D.B. Hartley and B.A. Thrush, Discussions Faraday Soc., 37, 64 (1964).

44) Robert Harris, J. Chem. Phys., 39, 978 (1963).

45) L. Landau and E. Teller, Phys. Z. Sowjetunion, 10, 34 (1936).

46) L.F. Keyser, F. Kaufman, and E.C. Zipf, to be published.

47) K. Sakurai and H.P. Broida, to be published.

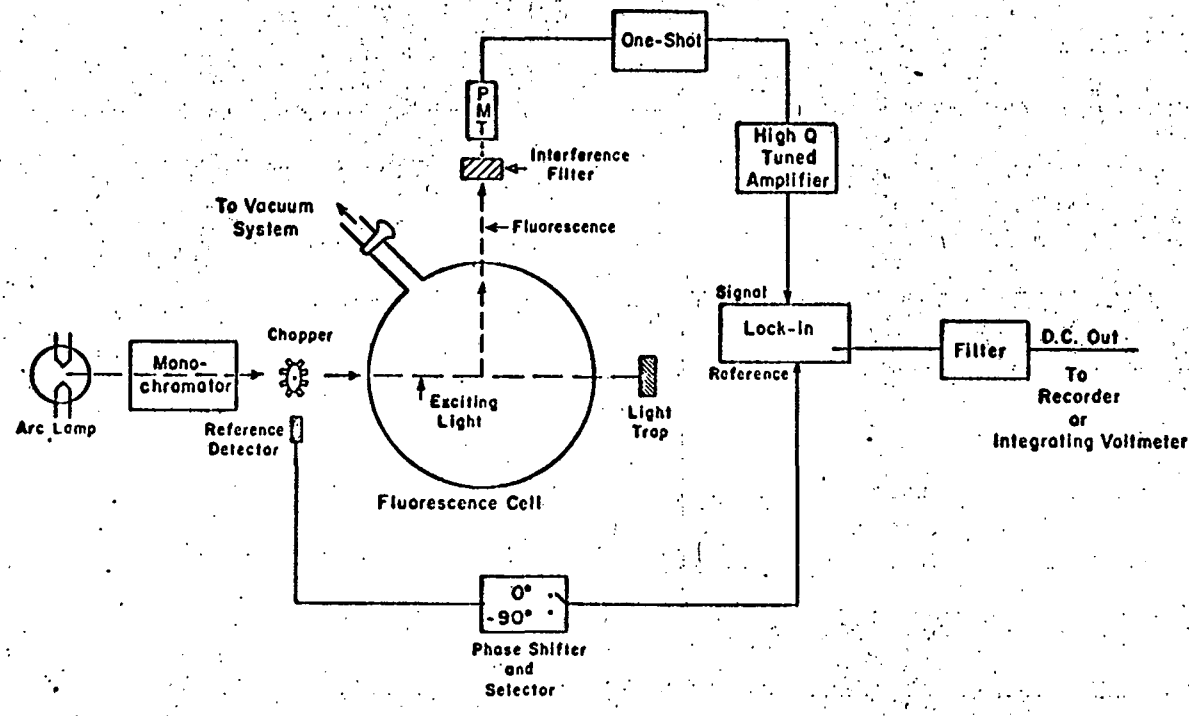
One-Shot
PMT
Interference Filter
High Q Tuned Amplifier
To Vacuum System
Fluorescence
Signal
Lock-In
Filter
D.C. Out
To Recorder or Integrating Voltmeter
Chopper
Mono-chromator
Arc Lamp
Reference Detector
Exciting Light
Light Trap
Reference
Fluorescence Cell
0°
-90°
Phase Shifter and Selector
XBL 685-734

Fig. 1

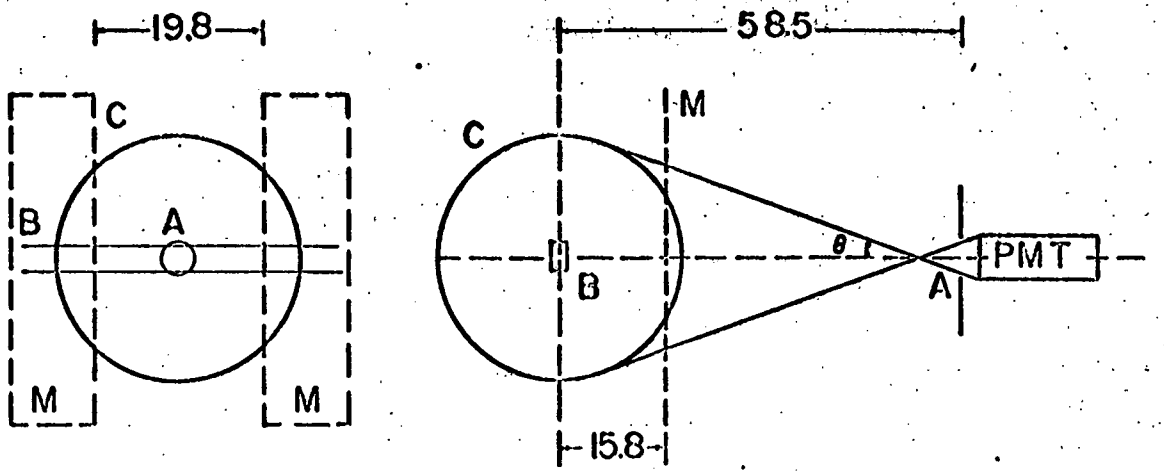

Fig. 2

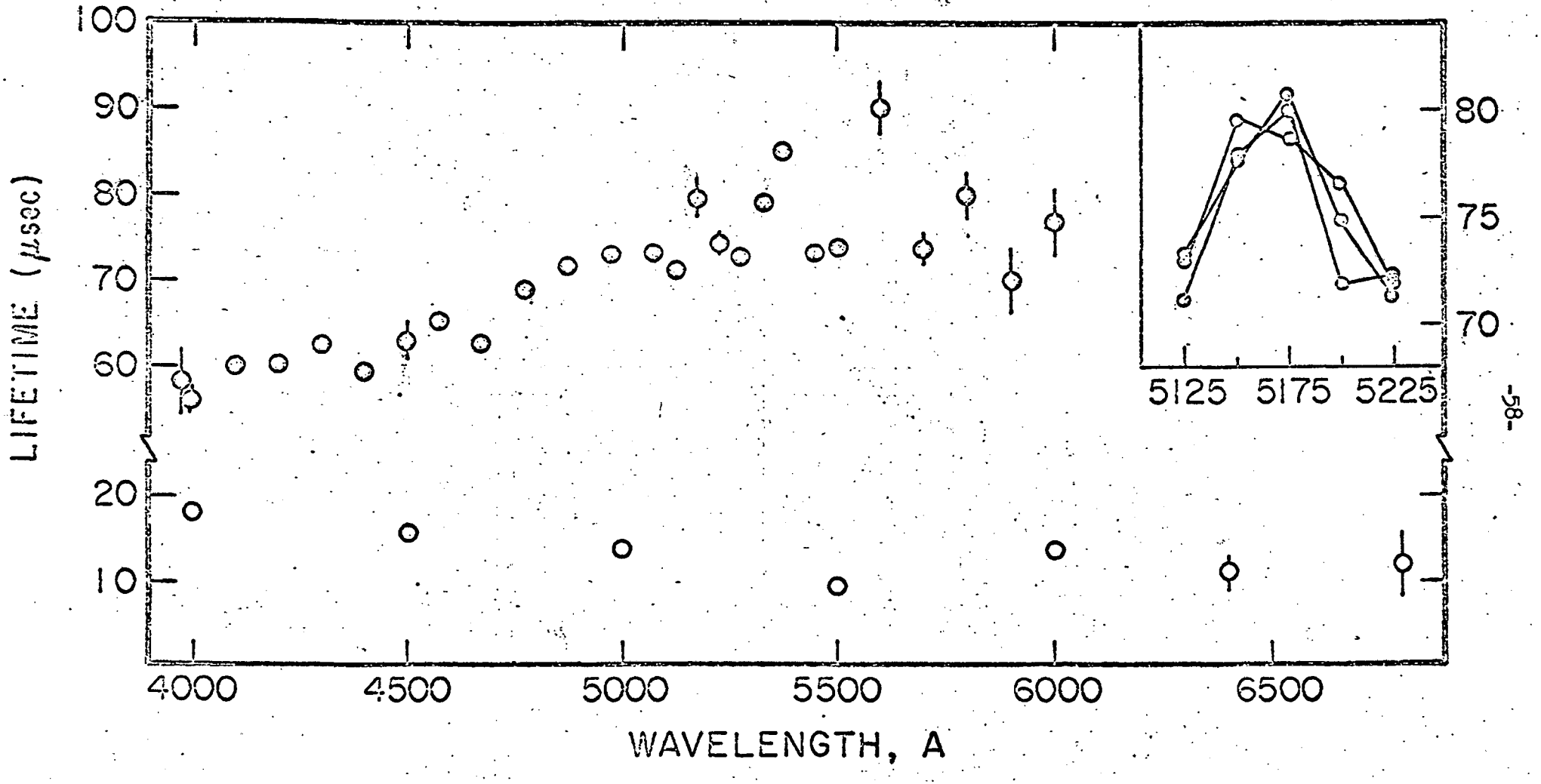
LIFETIME (μsec)
100
90
80
70
60
20
10
4000
4500
5000
5500
6000
6500
WAVELENGTH, A
80
75
70
5125
5175
5225

Fig. 3

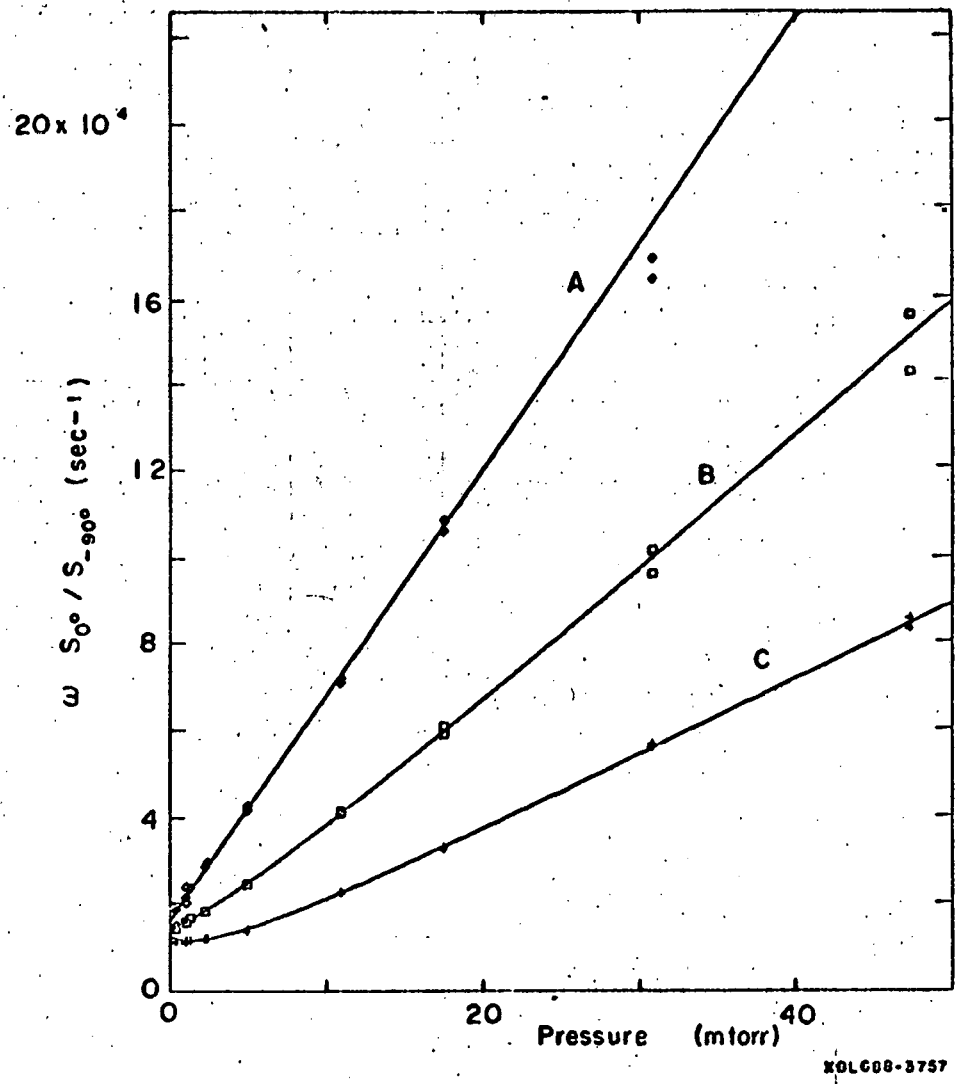
20 x 10⁻⁴
16
12
8
4
0
ω S0° / S-90° (sec-1)
A
B
C
0
20
40
Pressure (mtorr)
XDL608-3757

Fig. 4

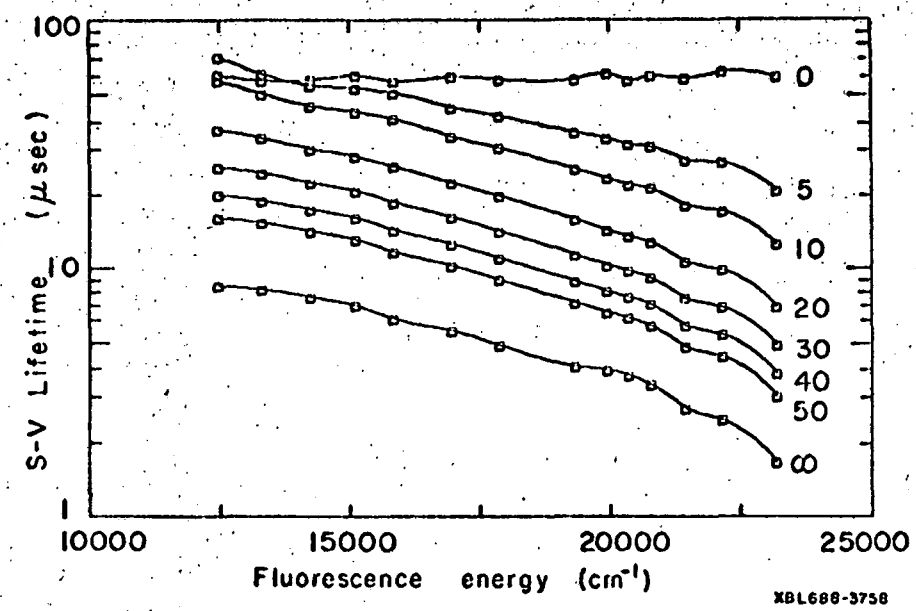
100
10
1
S-V Lifetime (μsec)
10000
15000
20000
25000
Fluorescence energy (cm⁻¹)
0
5
10
20
30
40
50
∞
XBL688-3758

Fig. 5 (a)

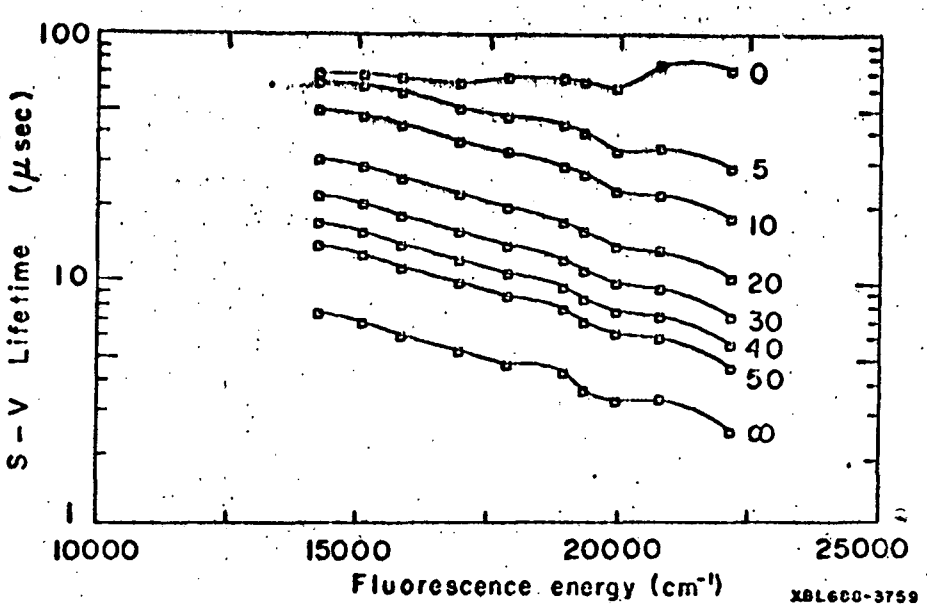
100
10
1
S-V Lifetime (μsec)
10000
15000
20000
25000
Fluorescence energy (cm⁻¹)
0
5
10
20
30
40
50
∞
XBL6CC-3759

Fig. 5(b)

5.b

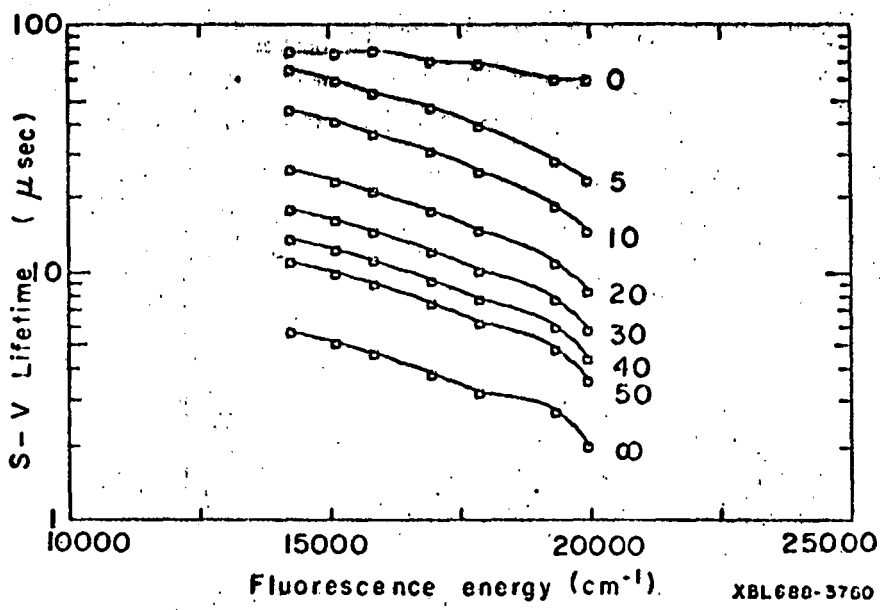
100
10
1
S-V Lifetime (μsec)
0
5
10
20
30
40
50
∞
10000
15000
20000
25000
Fluorescence energy (cm⁻¹)
XBL680-3760

Fig. 5 (c)

5c

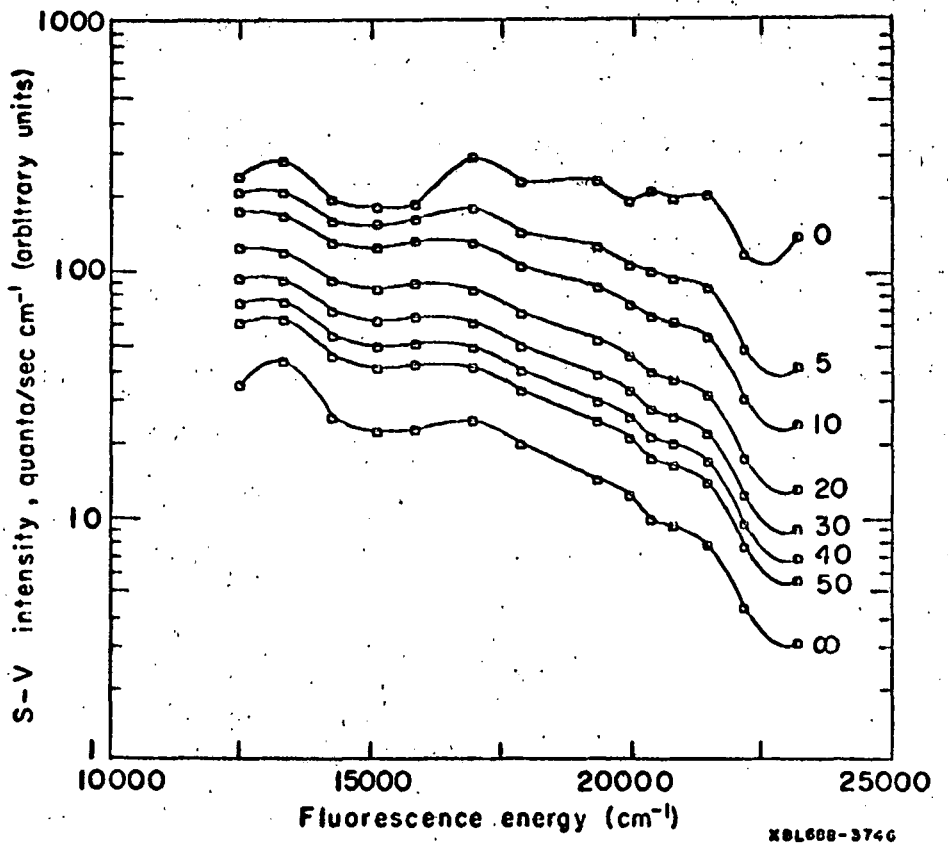
1000
100
10
1
S-V intensity, quanta/sec cm⁻¹ (arbitrary units)
10000
15000
20000
25000
Fluorescence energy (cm⁻¹)
0
5
10
20
30
40
50
∞
XBL688-3746

Fig. 6 (a)

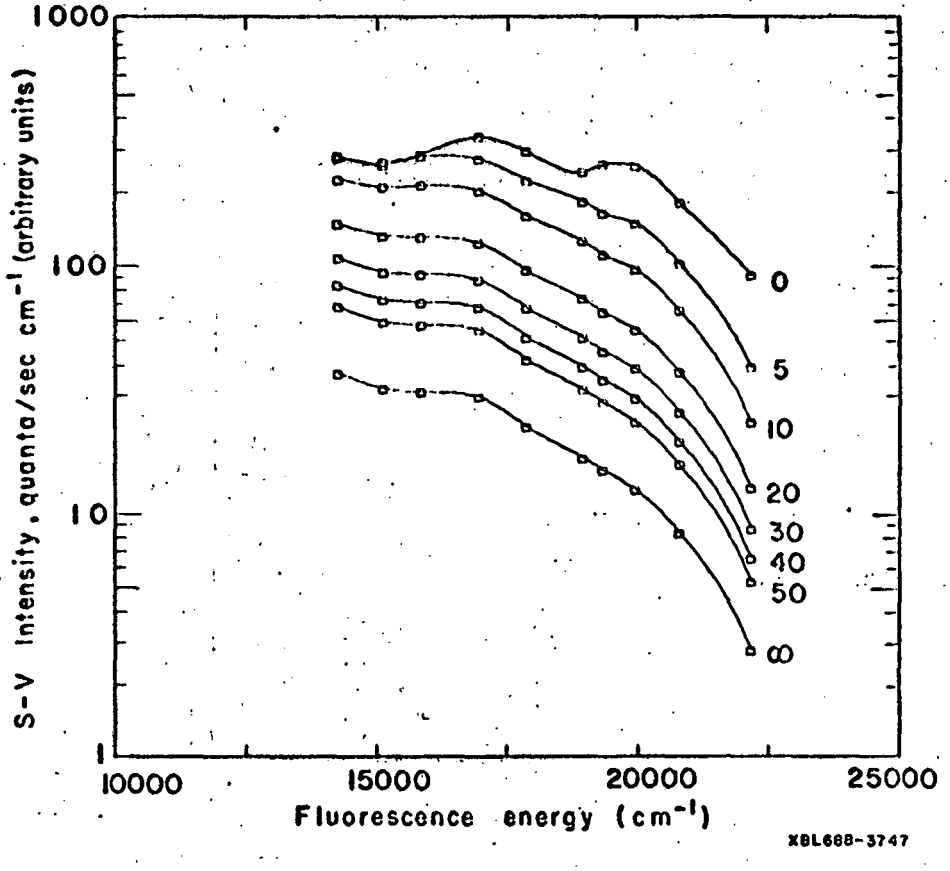
1000
100
10
1
S-V Intensity, quanta/sec cm⁻¹ (arbitrary units)
10000
15000
20000
25000
Fluorescence energy (cm⁻¹)
0
5
10
20
30
40
50
∞
XBL668-3747

Fig. 6 (b)

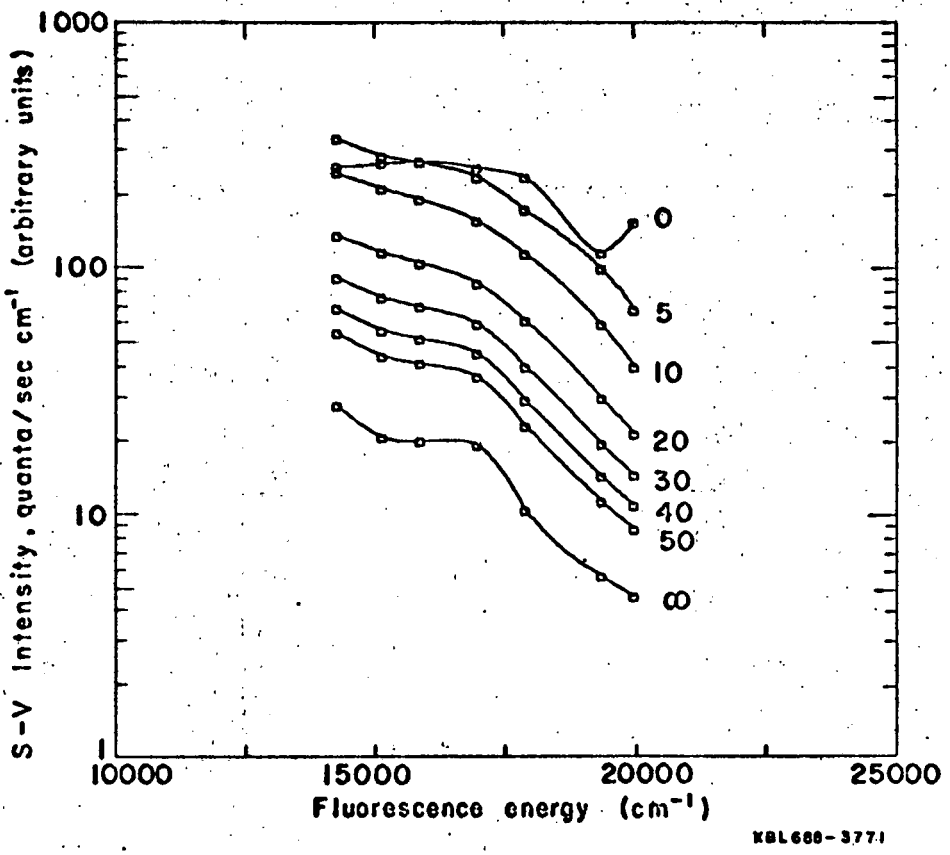
1000
100
10
1
S-V Intensity, quanta/sec cm⁻¹ (arbitrary units)
10000
15000
20000
25000
Fluorescence energy (cm⁻¹)
0
5
10
20
30
40
50
∞
XBL668-3771

Fig. 6 (c)

6C

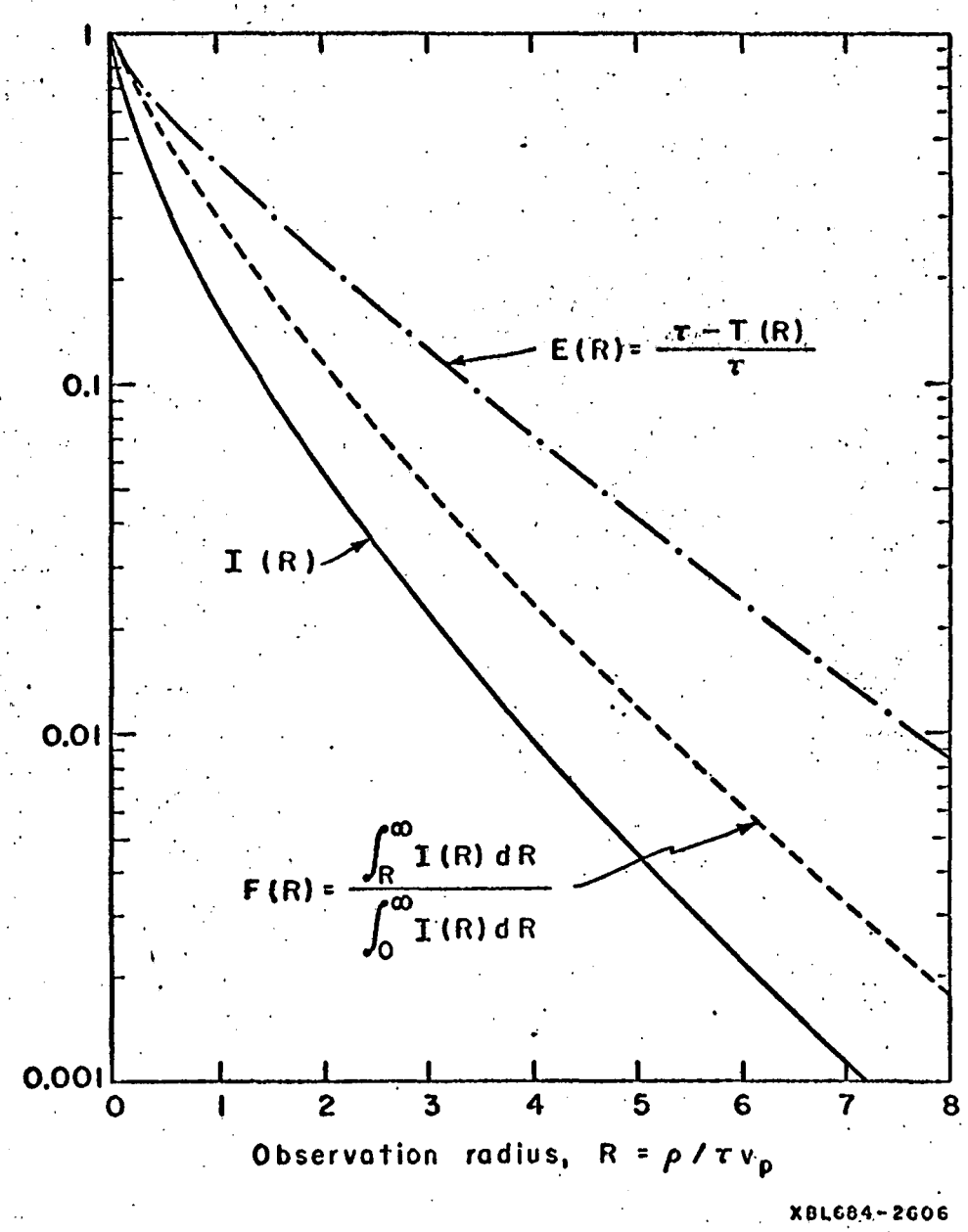
1
0.1
0.01
0.001
0
1
2
3
4
5
6
7
8
E(R)= τ − T(R) / τ
I (R)
F(R) = ∫_R^∞ I(R) dR / ∫_0^∞ I(R) dR
Observation radius, R = ρ / τ v_ρ
XBL684-2606

Fig. 7

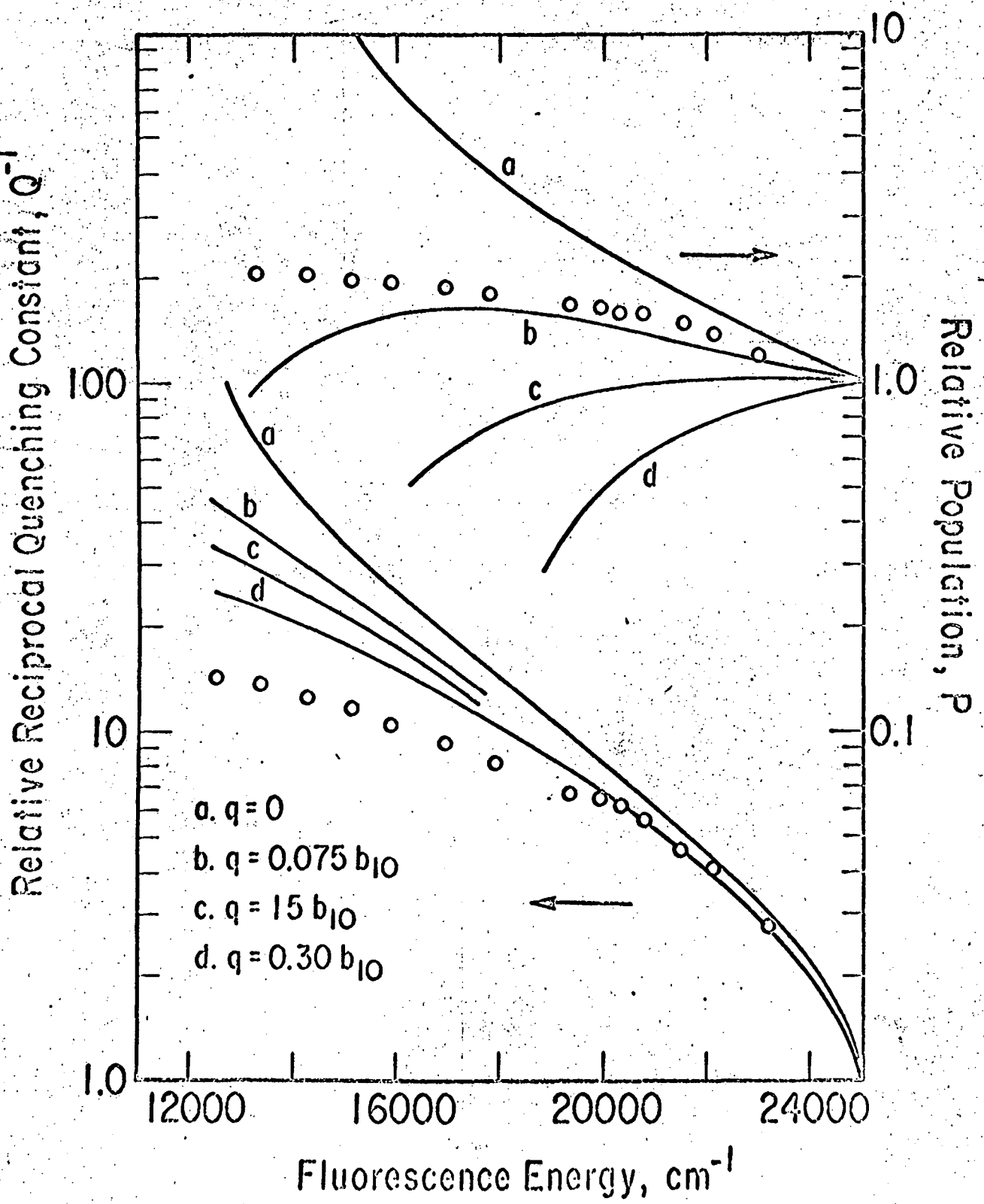
Relative Reciprocal Quenching Constant, Q^{-1}
Relative Population, P
Fluorescence Energy, cm^{-1}
100
10
1.0
10
1.0
0.1
12000
16000
20000
24000
a
b
c
d
a. q = 0
b. q = 0.075 b_{10}
c. q = 15 b_{10}
d. q = 0.30 b_{10}

Fig. 8

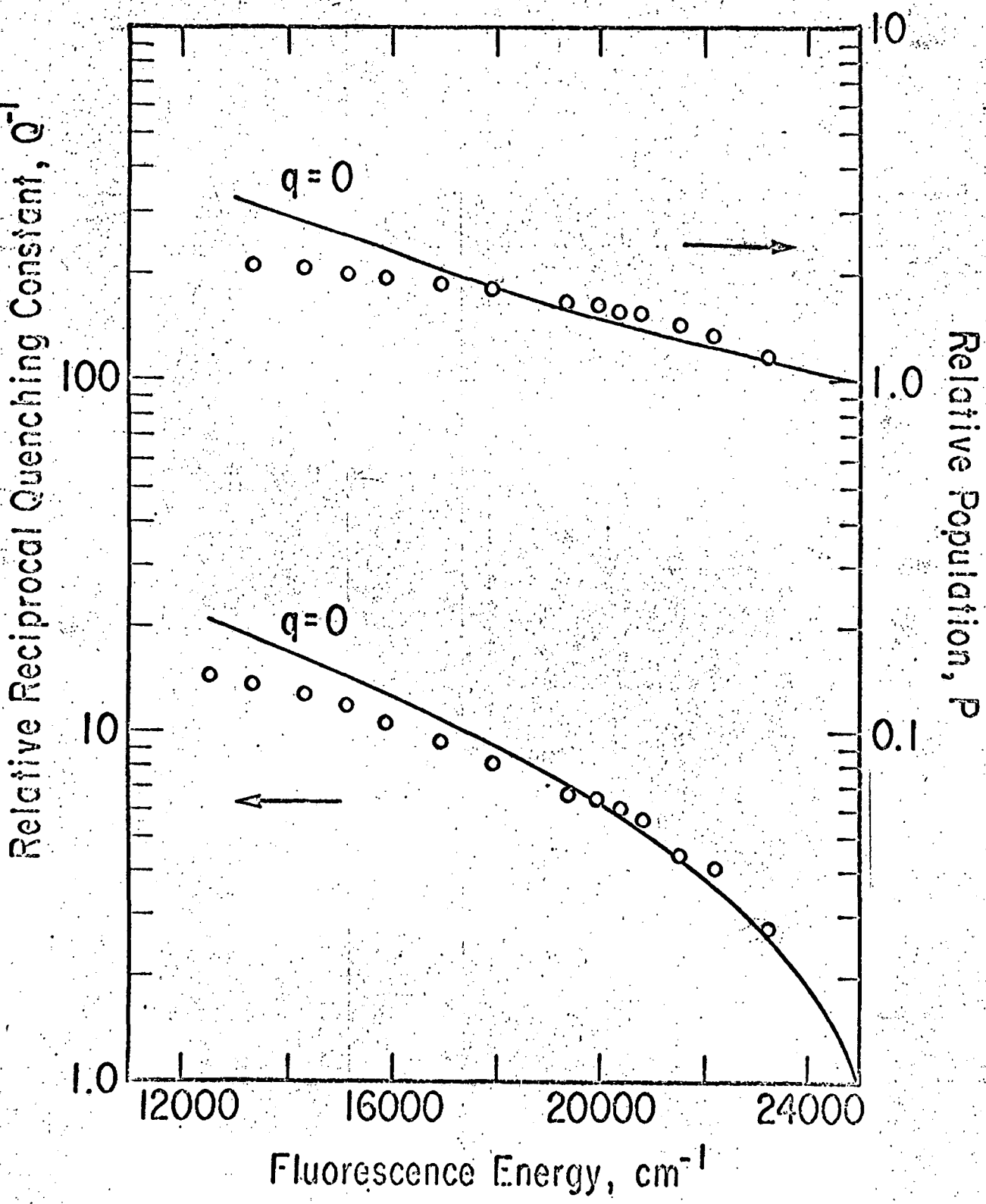
Relative Reciprocal Quenching Constant, Q^{-1}
Relative Population, P
Fluorescence Energy, cm^{-1}
q=0
q=0
100
10
1.0
10
1.0
0.1
12000
16000
20000
24000

Fig. 9

TECHNICAL INFORMATION DIVISION
LAWRENCE RADIATION LABORATORY
UNIVERSITY OF CALIFORNIA
BERKELEY, CALIFORNIA 94720